Large-Scale Structure Observations

Lecture 2

Will Percival

Cosmology from surveys

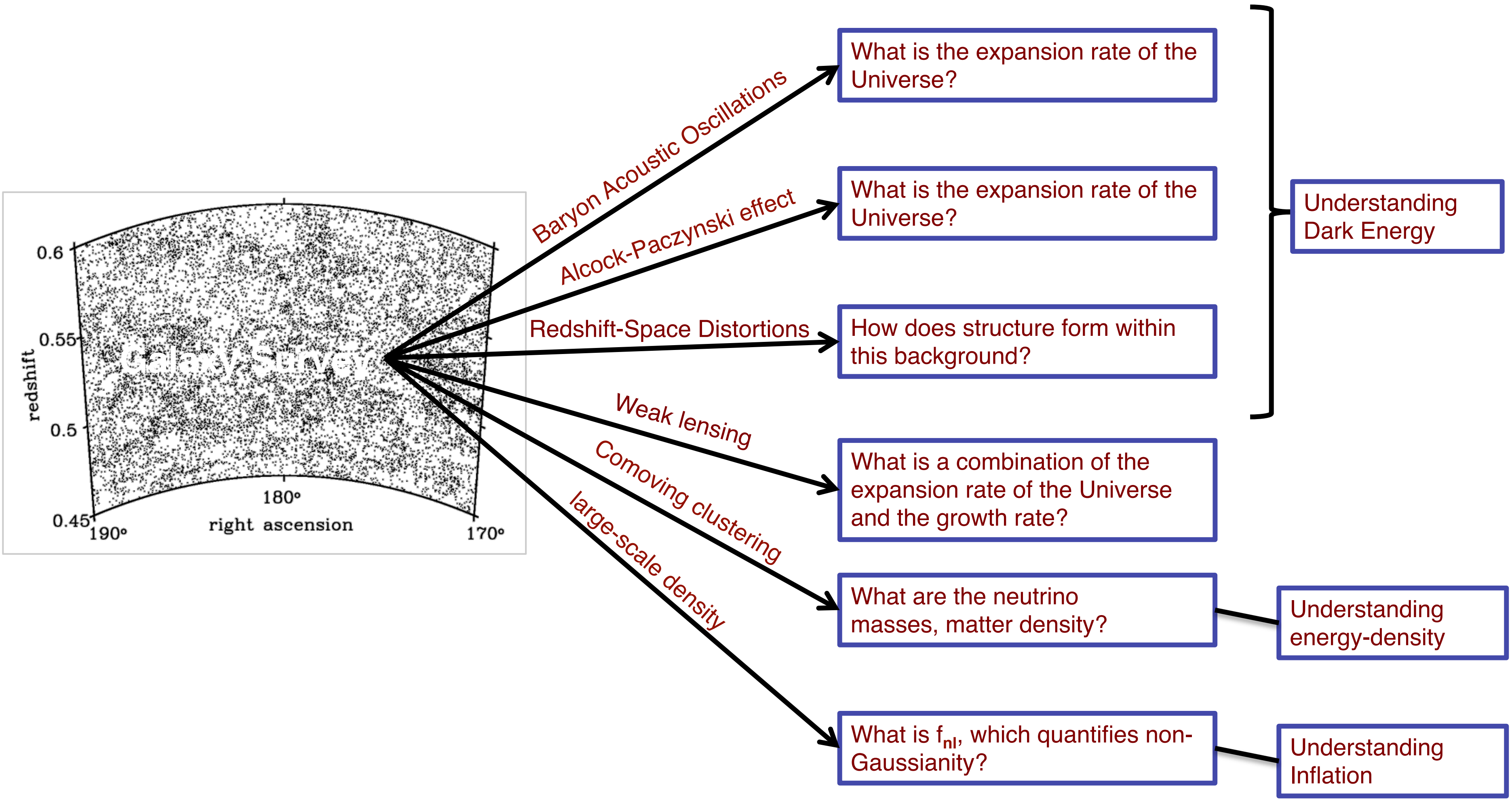

Redshift-space distortions

Comoving velocities

Locally, galaxies act as test particles in the flow of matter

On large-scales, the distribution of galaxy velocities is unbiased if galaxies fully sample the velocity field

expect a small peak velocity-bias due to motion of peaks in Gaussian random fields differing from that of the mass

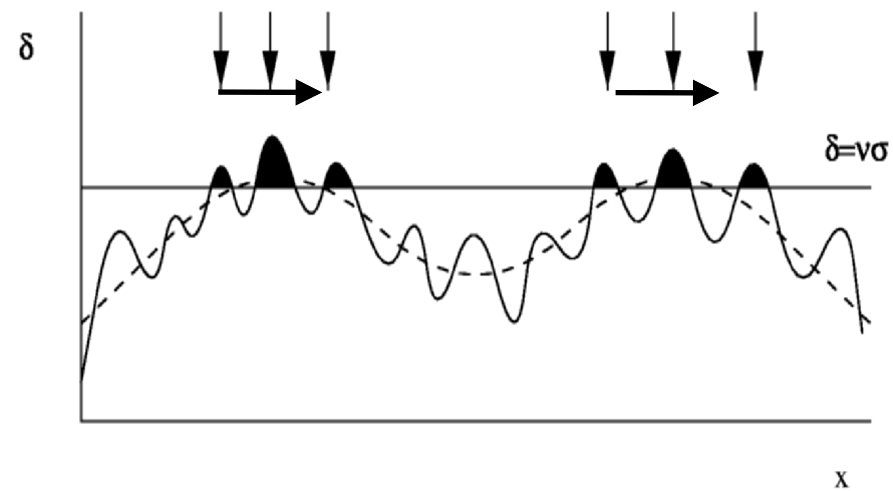

Redshift-Space Distortions

When making a 3D map of the Universe the radial distance is usually obtained from a redshift assuming Hubble's law; this differs from the real-space because of its peculiar velocity:

$$\vec{s}(r) = \vec{r} - v_r(r)\frac{\vec{r}}{r}$$

Where **s** and **r** are positions in redshift- and real-space and v_r is the peculiar velocity in the radial direction

Two key regimes of interest

linear flow

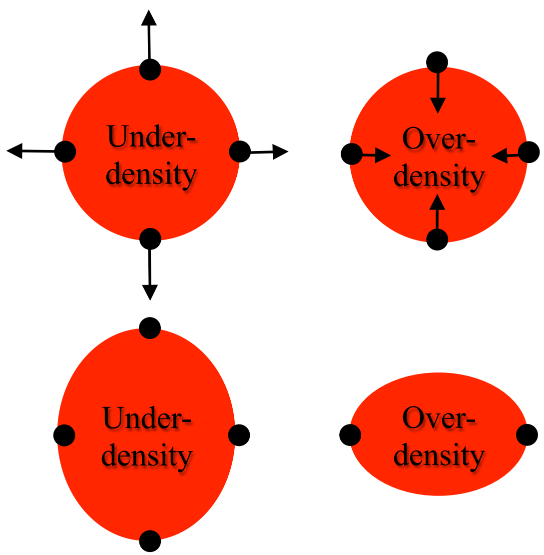

Power is enhanced
on large-scales

non-linear
structure

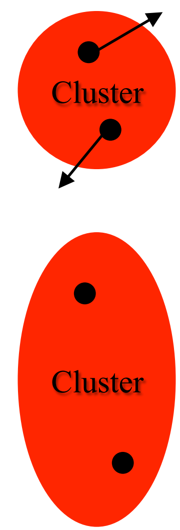

Actual
shape

Apparent
shape
(viewed from
below)

Power is suppressed
on small-scales

Fingers-of-God clearly visible in maps

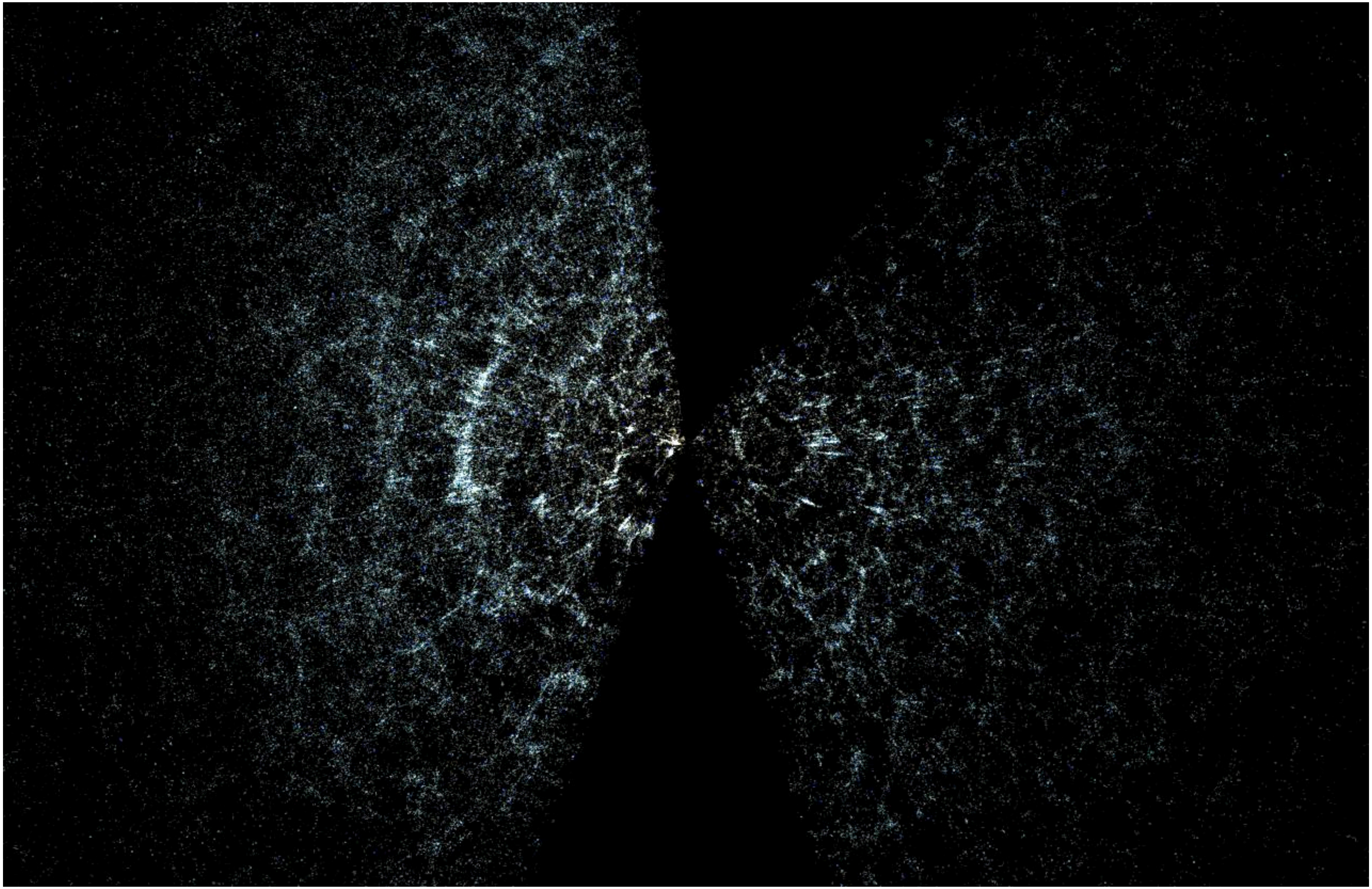

Image of SDSS, from U. Chicago

Linear plane-parallel redshift-space

Transition from real to redshift space, with peculiar velocity v **in units of the Hubble flow**

$$\mathbf{s} = \mathbf{r} + v_{\rm los}\hat{\mathbf{r}}_{\rm los}$$

$$\mu = cos(\alpha)$$
$$\theta = \nabla \cdot \mathbf{u}$$

Jacobian for transformation

$$\frac{d^3s}{d^3r} = \left(1 + \frac{v_{\rm los}}{r_{\rm los}}\right)^2 \left(1 + \frac{dv_{\rm los}}{dr_{\rm los}}\right)$$

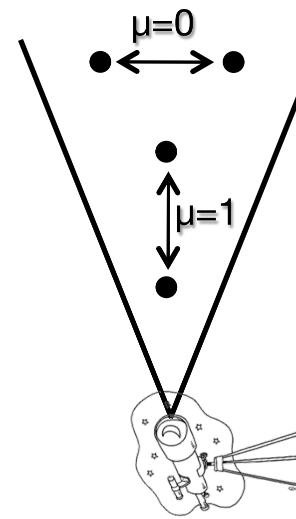

Conservation of galaxy number

$$n^r(\mathbf{r})d^3r = n^s(\mathbf{s})d^3s \qquad 1 + \delta_g^s = (1 + \delta_g^r)\frac{d^3r}{d^3s}\frac{\bar{n}^r(\mathbf{r})}{\bar{n}^s(\mathbf{s})}$$

Trick to understand velocity field derivative

$$\frac{\partial v_{\rm los}}{\partial r_{\rm los}} = \left(\frac{\partial}{\partial r_{\rm los}}\right)^2 \nabla^{-2}\theta = \left(\frac{k_{\rm los}}{k}\right)^2 \theta = \mu^2\theta, \;\; \theta = \nabla \cdot \mathbf{v}$$

Gives to first order

$$\delta_g^s = \delta_g^r - \mu^2\theta$$

Kaiser 1987, MNRAS, 227, 1

what do linear z-space distortions measure?

linear scales,

$$\begin{aligned}\delta_g^s(\mu) &= \delta_g + \mu^2\theta \\ P_g^s(\mu) &= \langle|\delta_g + \mu^2\theta|^2\rangle \\ &= P_{gg} + 2\mu^2 P_{g\theta} + \mu^4 P_{\theta\theta}\end{aligned}$$

$$\begin{aligned}\mu &= cos(\alpha) \\ \theta &= \nabla \cdot \mathbf{u}\end{aligned}$$

Galaxy-galaxy power

Velocity-velocity power

Galaxy-velocity divergence cross power

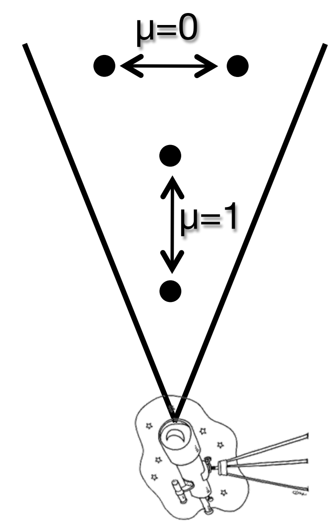

In linear regime

$$\delta_g = b\delta(\mathrm{mass}), \quad \theta = -f\delta(\mathrm{mass}), \quad f \equiv \frac{d\ln G}{d\ln a}$$

Linear growth rate

So, the simplest model for the power spectrum is

$$P_g^s(k,\mu) = \left[b + \mu^2 f\right]^2 P_{\mathrm{mass}}(k)$$

Kaiser 1987, MNRAS, 227, 1

Modeling redshift space distortions

Include model for both “regimes”

$$P_g^s(k,\mu) = \left[P_{gg}(k) + 2\mu^2 P_{g\theta}(k) + \mu^4 P_{\theta\theta}(k)\right] F(k,\mu^2)$$

Note that non-linear model is not necessarily more accurate then the linear one. If we assume linear bias

$$P_g^s(k,\mu) = P_m^r(k)\left[b^2 + 2\mu^2 f b + \mu^4 f^2\right] F(k,\mu^2)$$

On small scales, galaxies lose all knowledge of initial position. If pairwise velocity dispersion has an exponential distribution (superposition of Gaussians), then we get this damping term for the power spectrum.

$$F(k,\mu^2) = (1 + k^2\mu^2\sigma_p^2/2)^{-1}$$

Modeling redshift space distortions

Alternative for the data is to try to "correct" the data by "collapsing the clusters"

- Velocity dispersion of the Luminous Red Galaxies (LRGs) shifts them along the line of sight by ~ 9 h^{-1}Mpc, and the distribution of intrahalo velocities has long tails.
- Use an asymmetric "friends-of-friends" (FOF) finder to match galaxies in the same clusters, and collapse to spherical profile
- Parameters of FOF calculated by matching simulations

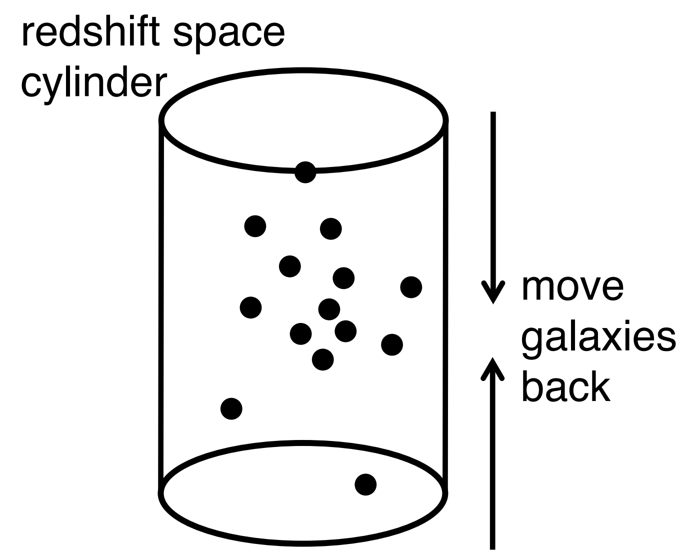

Reid et al. 2008, arXiv:0811.1025; Reid et al. 2009, arXiv:0907.1659

Cosmology improved with RSD

- Anisotropic clustering allows huge improvement on w!
  - w = -0.95 ± 0.25 (WMAP + $D_V(0.57)/r_s$)
  - w = -0.88 ± 0.055 (WMAP + anisotropic)
- Provides a number of GR tests

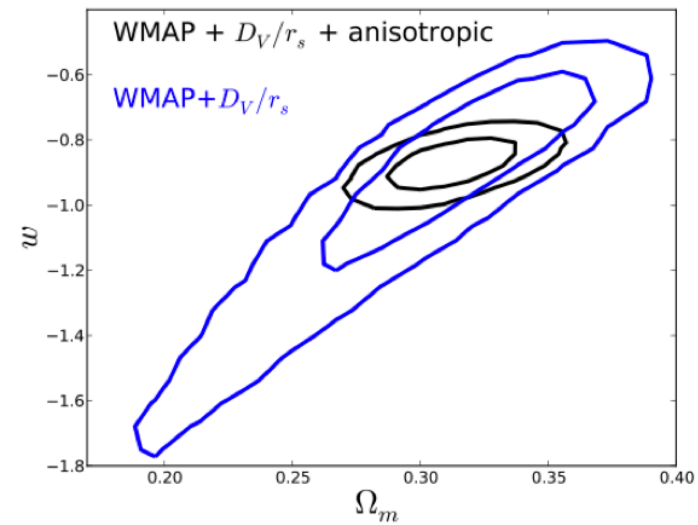

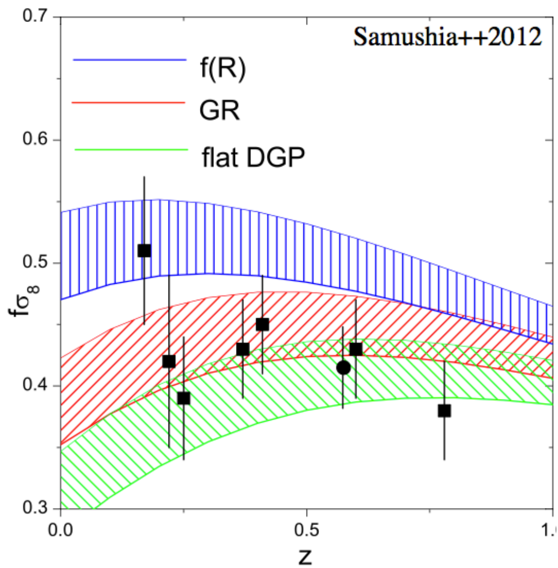

Samushia et al. 2012; arXiv:1206.5309

Anisotropic statistics

Legendre moments – power spectrum

Remember that, in linear theory and the plane-parallel limit, we have a angular dependence

$$P^s_g(k,\mu) = P_{gg}(k) + 2\mu^2 P_{g\theta}(k) + \mu^4 P_{\theta\theta}(k)$$

Then we can consider the orthogonal Legendre multipoles of P

$$P^s_\ell(k) \equiv \frac{2\ell+1}{2}\int_{-1}^{+1} d\mu \; P^s_g(k,\mu) L_\ell(\mu)$$

where

$$\begin{aligned} L_0(\mu) &= 1 \\ L_2(\mu) &= (3\mu^2-1)/2 \\ L_4(\mu) &= (35\mu^4 - 30\mu^2 + 3)/8 \end{aligned}$$

Such that

$$\begin{pmatrix} P^s_0(k) \\ P^s_2(k) \\ P^s_4(k) \end{pmatrix} = \begin{pmatrix} 1 & 2/3 & 1/5 \\ 0 & 4/3 & 4/7 \\ 0 & 0 & 8/35 \end{pmatrix} \begin{pmatrix} P_{gg}(k) \\ P_{g\theta}(k) \\ P_{\theta\theta}(k) \end{pmatrix}$$

$$P^s(k) = P^s_0(k)L_0(\mu) + P^s_2(k)L_2(\mu) + P^s_4(k)L_4(\mu)$$

Legendre moments – power spectrum

These can then be manipulated leading to cosmological information

From the monopole, quadrupole and hexadecapole we obtain:

$$\begin{pmatrix} P_{gg}(k) \\ P_{g\theta}(k) \\ P_{\theta\theta}(k) \end{pmatrix} = \begin{pmatrix} 1 & -1/2 & 3/8 \\ 0 & 3/4 & -15/8 \\ 0 & 0 & 35/8 \end{pmatrix} \begin{pmatrix} P_0^s(k) \\ P_2^s(k) \\ P_4^s(k) \end{pmatrix}$$

The ratio of quadrupole to monopole gives:

$$\frac{P_2^s(k)}{P_0^s(k)} = \frac{\frac{4}{3}bf + \frac{4}{7}f^2}{b^2 + \frac{2}{3}fb + \frac{1}{5}f^2}$$

A more complicated formula can be used to eliminate bias:

$$P_{\theta\theta}(k) = \frac{7}{48}\left[5(7P_0^s + P_2^s) - \sqrt{35}[35(P_0^s)^2 + 10P_0^s P_2^s - 7(P_2^s)^2]^{1/2}\right]$$

e.g. Percival & White 2009; MNRAS 393, 297

Legendre moments – correlation function

The correlation function can similarly be decomposed into Legendre moments

$$\xi^s_\ell(r) = \frac{(2\ell+1)}{2}\int_{-1}^{+1} d\mu\ \xi^s(r,\mu)L_\ell(\mu)$$

$$\xi^s(r,\mu) = \sum_{\ell\ \mathrm{even}} L_\ell(\mu)\xi^s_\ell(r)$$

The first three even moments ξ_0, ξ_2, ξ_4 allow the full linear theory to be recovered

$$\begin{aligned}
\xi^s_0(r) &= (b^2 + \frac{2}{3}bf + \frac{1}{5}f^2)\xi^r(r) \\
\xi^s_2(r) &= (\frac{4}{3}bf + \frac{4}{7}f^2)[\xi^r(r) - \bar{\xi}^r(r)] \\
\xi^s_4(r) &= \frac{8}{35}f^2[\xi^r(r) + \frac{5}{2}\bar{\xi}^r(r) - \frac{7}{2}\bar{\bar{\xi}}^r(r)]
\end{aligned}$$

$$\bar{\xi}^r(r) \equiv 3r^{-3}\int_0^r \xi^r(r')r'^2\,dr' \qquad \bar{\bar{\xi}}^r(r) \equiv 5r^{-5}\int_0^r \xi^r(r')r'^4\,dr'$$

Hamilton 1992; ApJ 385, L5

The Alcock-Paczynski Effect

The Alcock-Paczynski Effect

- If the Universe is isotropic, clustering is same radial & tangential
- Stretching at a single redshift slice (for galaxies expanding with Universe) depends on

  $H^{-1}(z)$ (radial)

  $D_A(z)$ (angular)

- Analyze with wrong model -> see anisotropy
- AP effect measures $F = D_A(z)H(z)$
- RSD limits test to scales where can be modeled

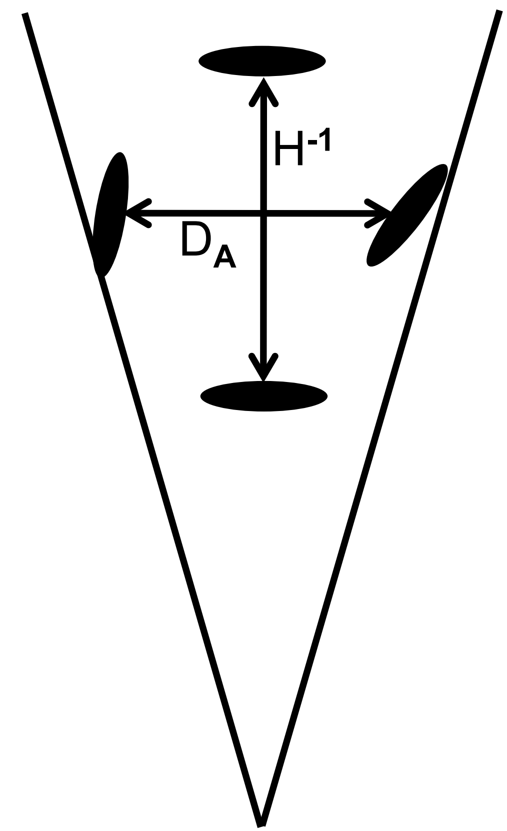

Fitting BAO along and across line-of-sight

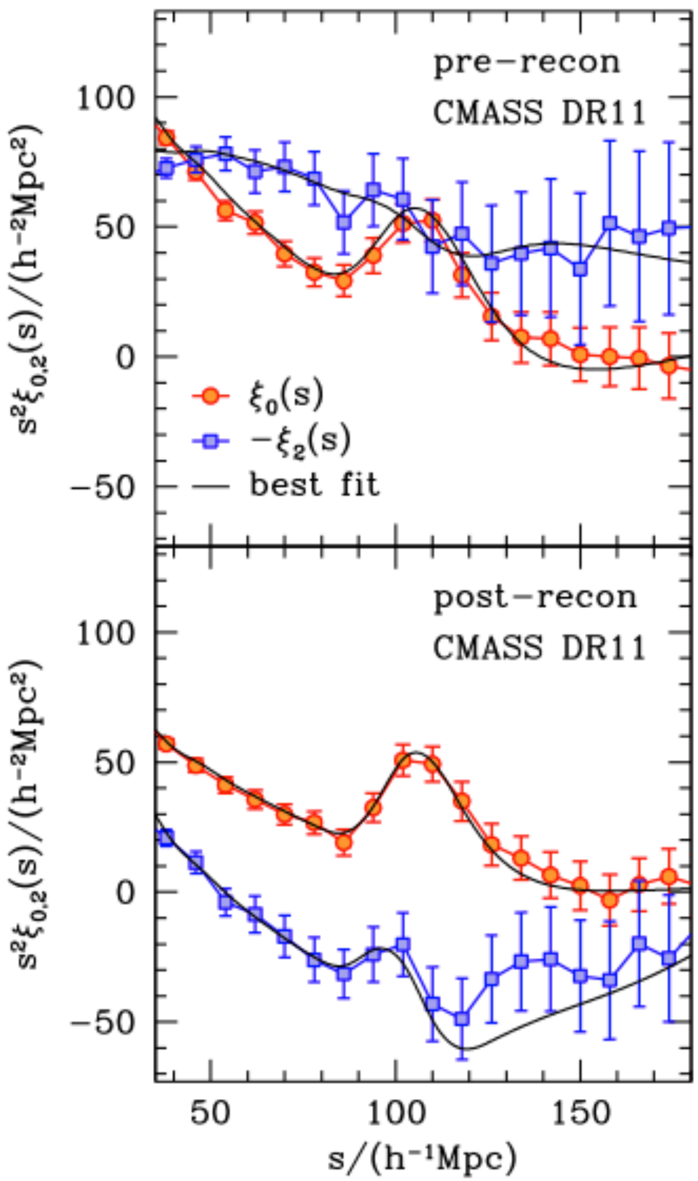

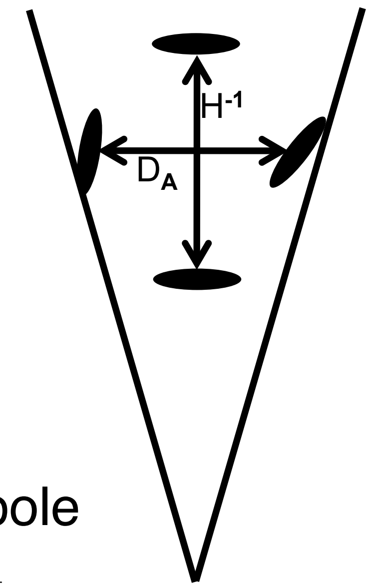

monopole

$$\xi_2^s(r) = \frac{3}{2}\int_{-1}^{+1} d\mu\ \xi^s(r,\mu)$$

quadrupole

$$\xi_2^s(r) = \frac{5}{2}\int_{-1}^{+1} d\mu\ \xi^s(r,\mu)\frac{3\mu^2-1}{2}$$

Anderson et al. 2013; arXiv:1312.4877

AP effect on monopole & quadrupole

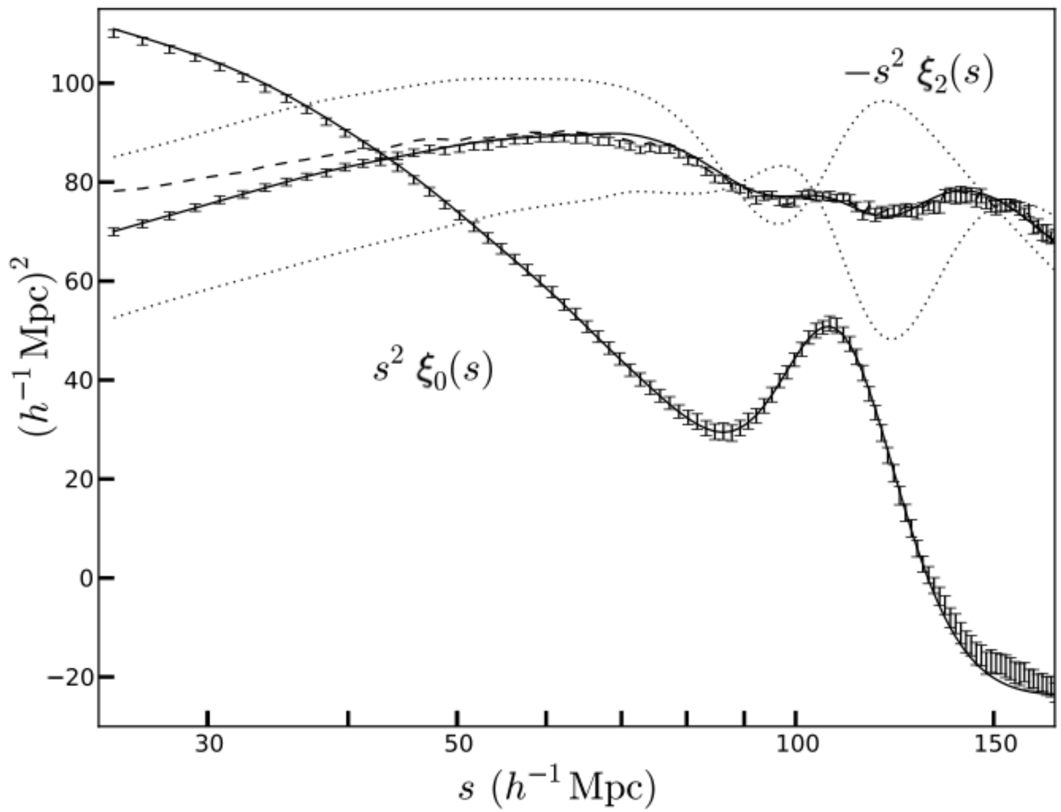

Varying F by 10%, while keeping peak position in monopole fixed

- AP moves ξ(r) in scale (left-right).
- Movement of BAO “bump” is clear.
- Shape of ξ(r) close to power law, so AP is very similar to amplitude shift (as RSD).
- Allows measurements of F & fσ_8 to be separated

Reid et al. 2012; arXiv:1203.6641

Anisotropic BAO fits to BOSS data

	$D_A(z)(r_s^{\rm fid}/r_s)$	$H(z)(r_s/r_s^{\rm fid})$	$\rho_{D_A H}$
	Before Reconstruction		
$(\xi_0(s), \xi_2(s))$	1367 ± 44	86.6 ± 6.2	0.65
$(\xi_\perp(s), \xi_\parallel(s))$	1379 ± 42	88.3 ± 5.1	0.52
	After Reconstruction		
$(\xi_0(s), \xi_2(s))$	1424 ± 43	95.4 ± 7.5	0.63
$(\xi_\perp(s), \xi_\parallel(s))$	1386 ± 36	90.6 ± 6.7	0.50
Consensus	1408 ± 45	92.9 ± 7.8	0.55

Anderson et al. 2013; arXiv:1303.4666

Anisotropic BAO measurements vs CMB

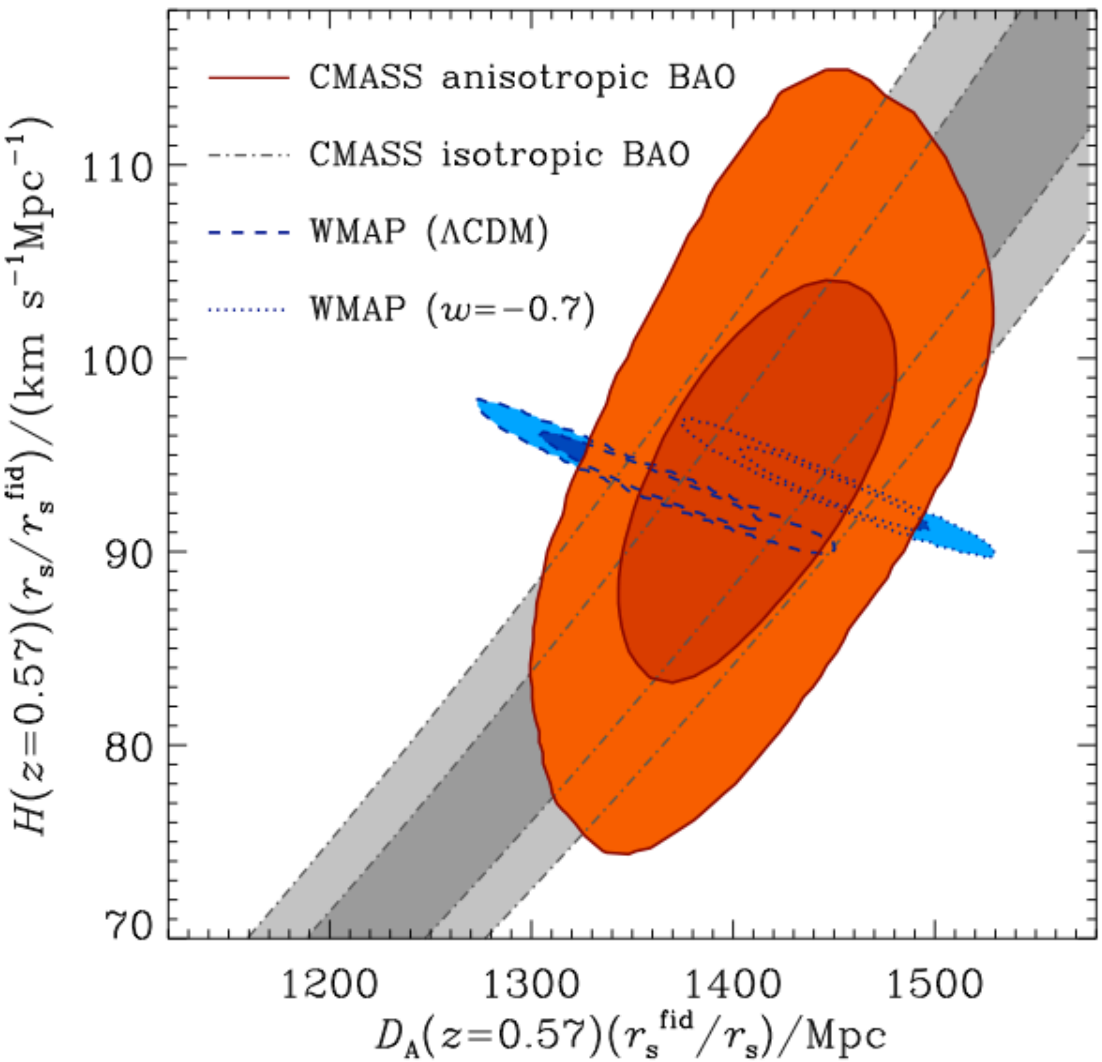

Anderson et al. 2013; arXiv:1303.4666

RSD and AP amplitude shift strongly correlated

We should allow for the coupling between the redshift-space distortions and the geometrical squashing caused by getting the geometry wrong. Effects are not perfectly degenerate

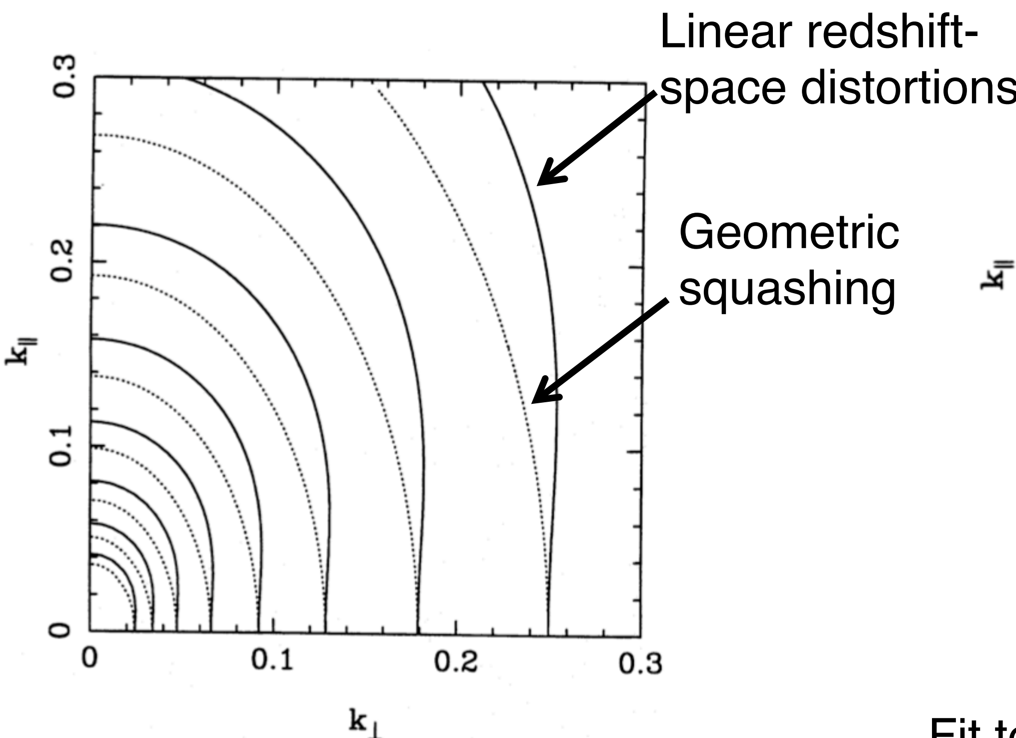

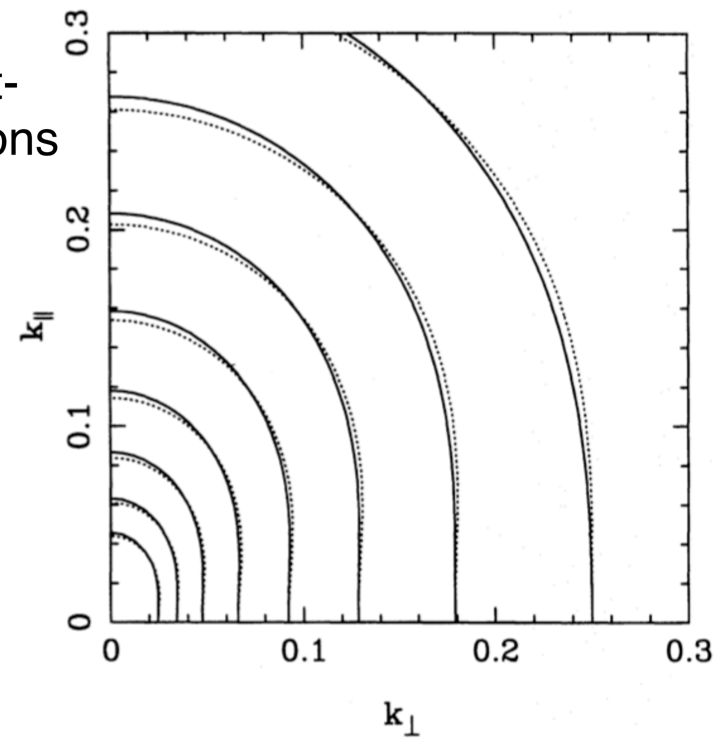

Fit to redshift-space distortions cannot mimic geometric squashing

Ballinger, Peacock & Heavens 1999, MNRAS, 282, 877

Degradation of RSD measurements by AP effect

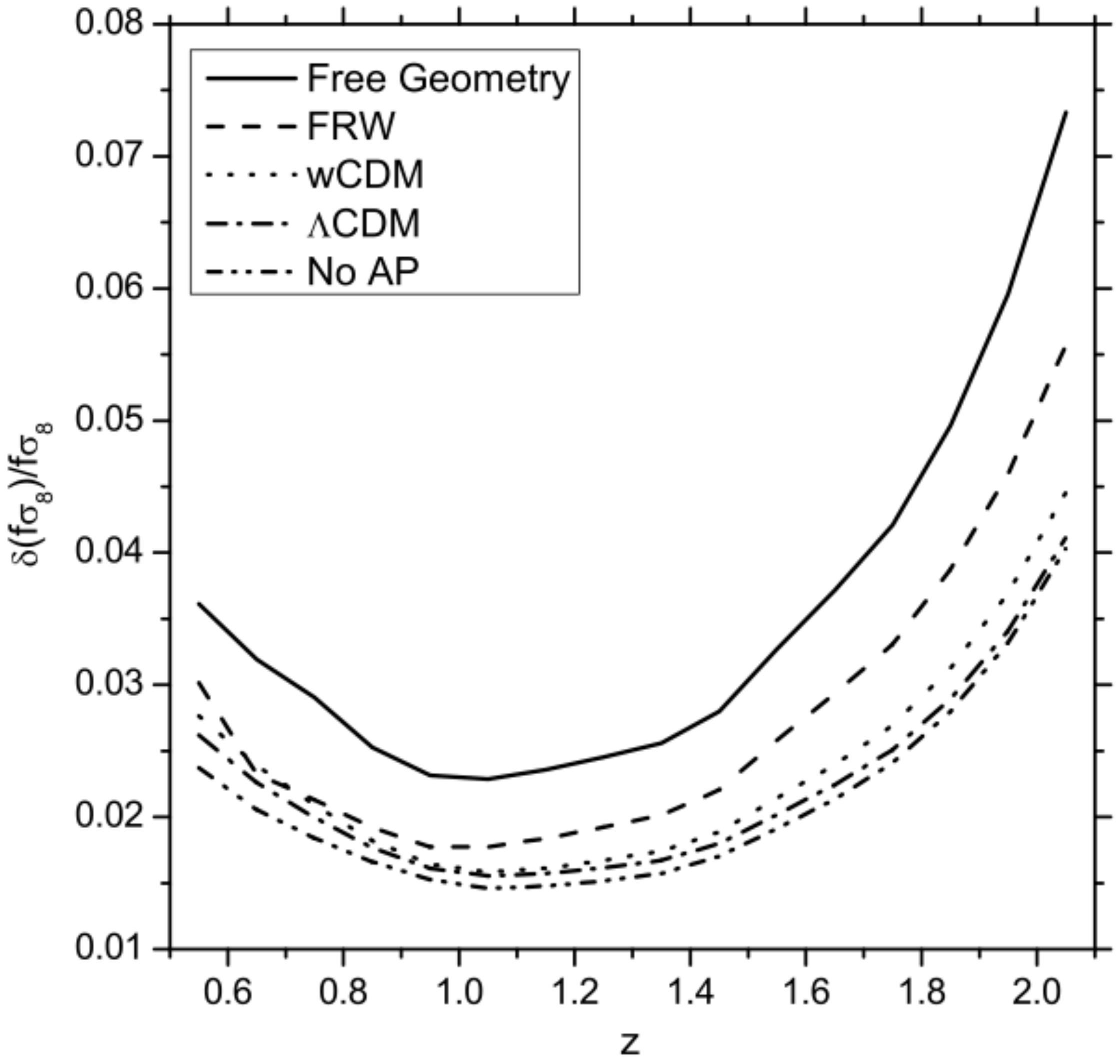

Samushia et al 2011, MNRAS 410, 1993

BOSS AP & RSD measurement degeneracy

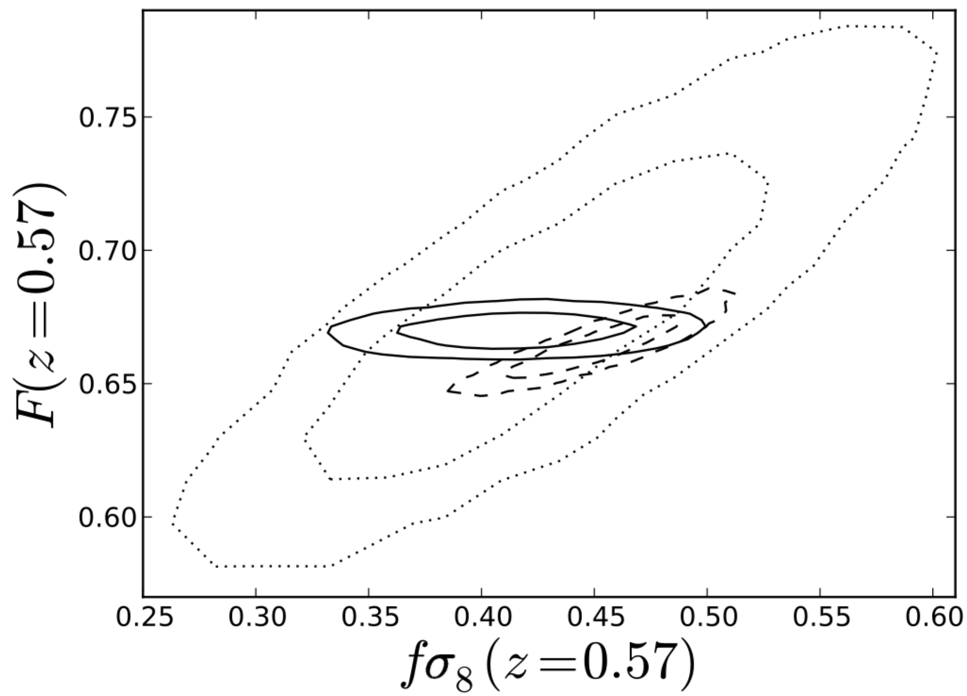

Dotted: free growth, geometry, ΛCDM prior on large-scale linear P(k) shape at z=0.57

Solid: F forced to match ΛCDM model

Dashed: WMAP ΛCDM+GR prediction

Reid et al. 2012; arXiv:1203.6641

BOSS F measurements in context

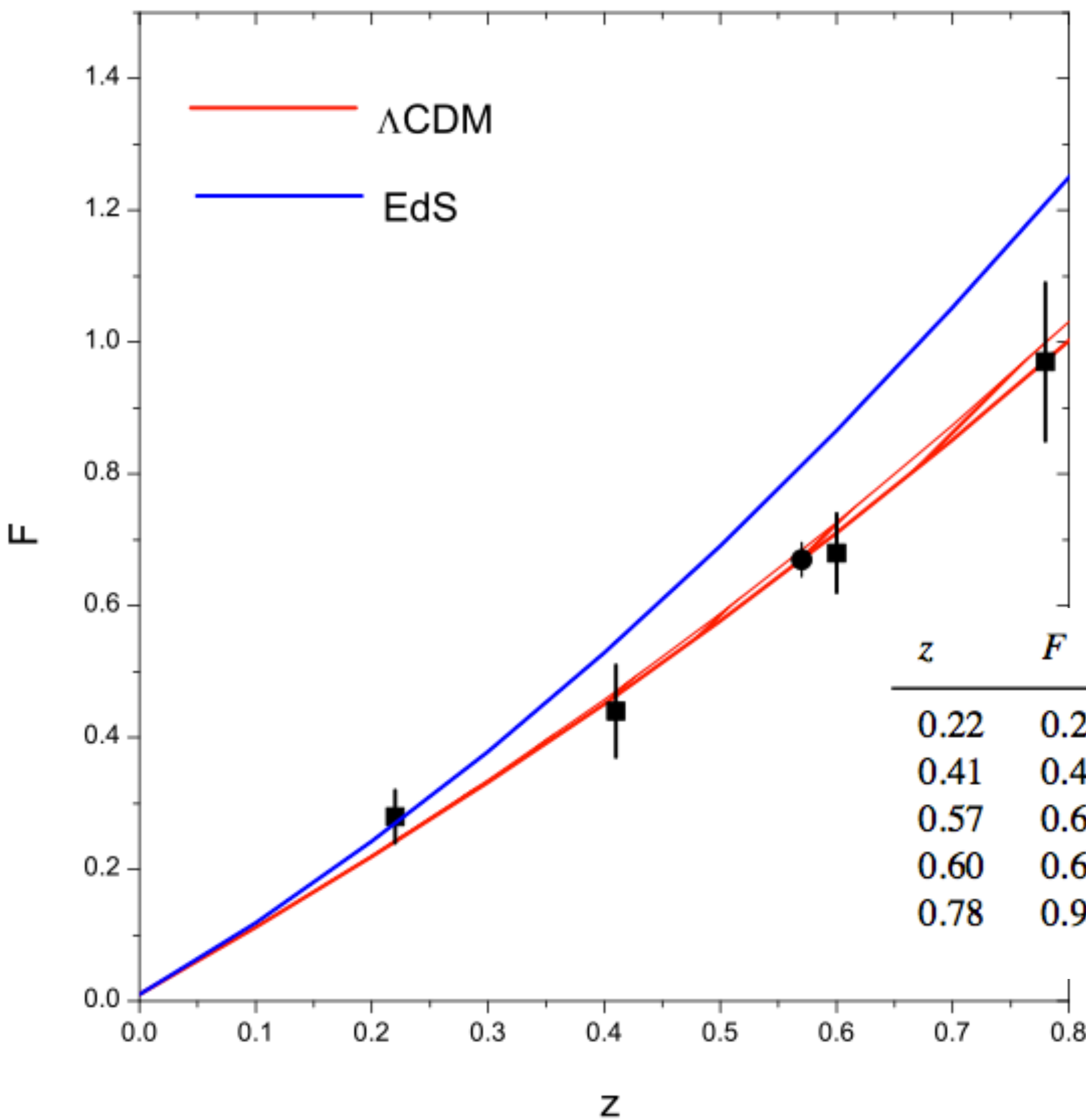

z	F	survey	reference
0.22	0.28 ± 0.04	WiggleZ	Blake, et al. (2011c)
0.41	0.44 ± 0.07	WiggleZ	Blake, et al. (2011c)
0.57	0.67 ± 0.026	BOSS	Reid et al. (2012)
0.60	0.68 ± 0.06	WiggleZ	Blake, et al. (2011c)
0.78	0.97 ± 0.12	WiggleZ	Blake, et al. (2011c)

Samushia et al. 2012; arXiv:1206.5309

BOSS RSD measurements in context

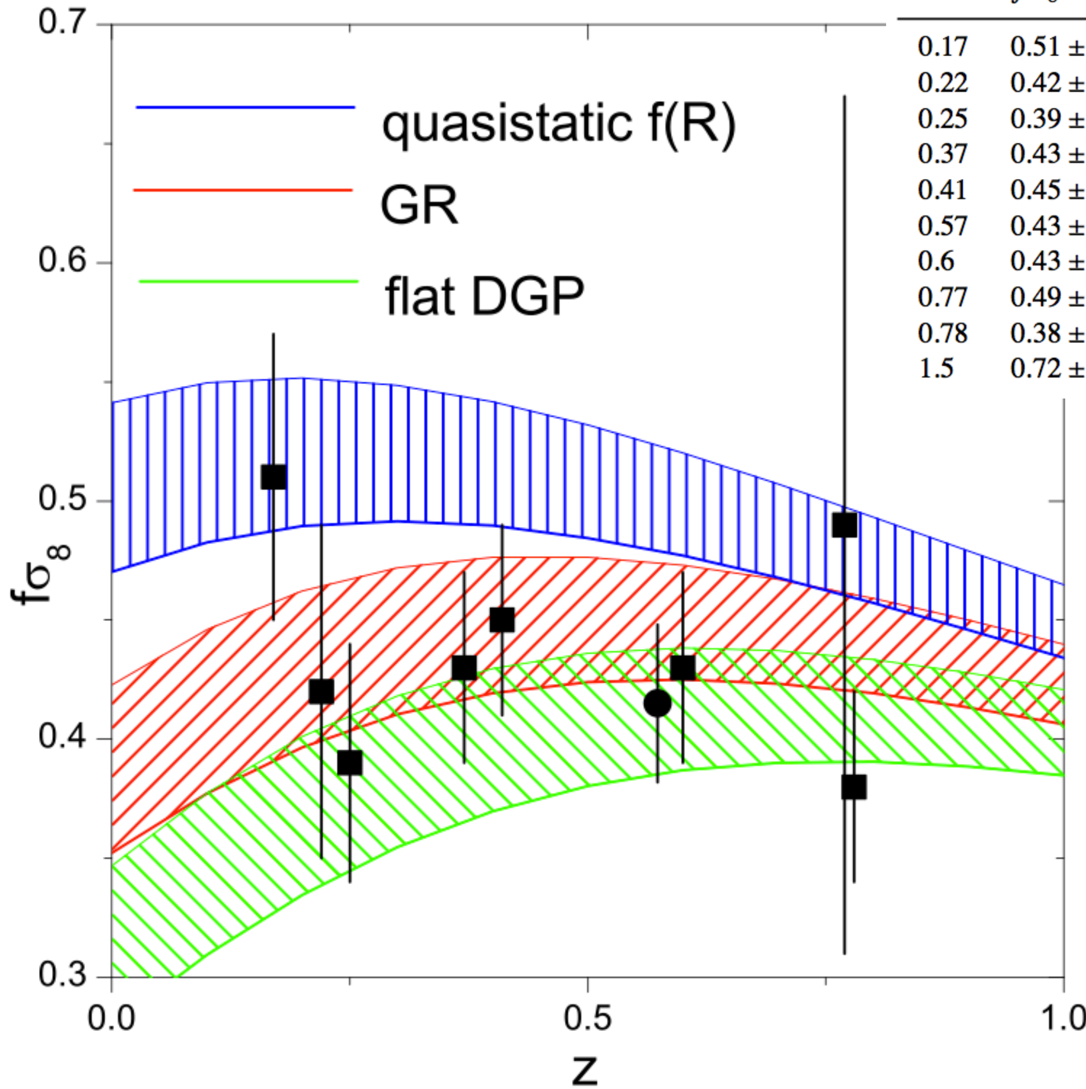

z	$f\sigma_8$	survey	reference
0.17	0.51 ± 0.06	2dFGRS	Percival et al. (2004)
0.22	0.42 ± 0.07	WiggleZ	Blake, et al. (2011b)
0.25	0.39 ± 0.05	SDSS	Samushia, Percival, & Raccanelli (2011)
0.37	0.43 ± 0.04	SDSS	Samushia, Percival, & Raccanelli (2011)
0.41	0.45 ± 0.04	WiggleZ	Blake, et al. (2011b)
0.57	0.43 ± 0.03	BOSS	Reid et al. (2012)
0.6	0.43 ± 0.04	WiggleZ	Blake, et al. (2011b)
0.77	0.49 ± 0.18	VVDS	Guzzo et al. (2007)
0.78	0.38 ± 0.04	WiggleZ	Blake, et al. (2011b)
1.5	0.72 ± 0.15	2SLAQ	da Angela et al. (2008)

Samushia et al. 2012; arXiv:1206.5309

The effect of AP uncertainty on RSD

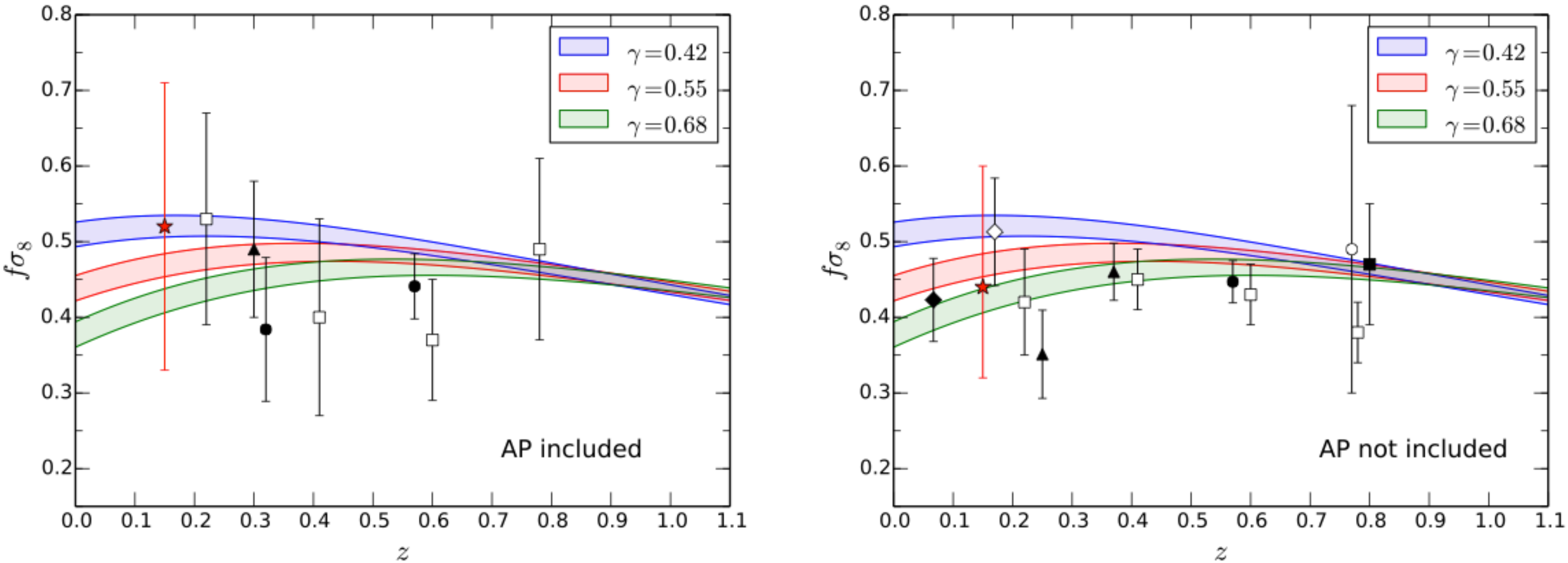

Howlett et al. 2014; arXiv:1409.3238

Primordial non-Gaussianity

Measuring primordial non-Gaussianity: f_{NL} g_{NL}

δ is sourced from a potential field **Φ**, whose form might not be Gaussian

$$\nabla^2\Phi(\mathbf{x}) = 4\pi G\delta(\mathbf{x})$$

$$\Phi(\mathbf{x}) \sim \phi(\mathbf{x}) + f_{NL}\phi^2(\mathbf{x}) + ...$$

skewness ~ f_{NL}
kurtosis ~ f_{NL}^2
...

ϕ is a Gaussian field. the non-linear terms in **Φ** make **Φ** non-Gaussian. This map completely specifies **Φ** statistics.

Salopek and Bond 1990;
Gangui, Lucchin, Matarrese, Mollerach 1994;
Komatsu and Spergel 2001

$$\Phi(\mathbf{x}) \sim \phi(\mathbf{x}) + g_{NL}\phi^3(\mathbf{x}) + ...$$

skewness ~ 0
kurtosis ~ g_{NL}
…

f_{NL} is not the only option for local potential fluctuations … you can go even further down this route …

Okamoto and Hu 2002;
Enqvist and Nurmi 2005

Non-local models introduce non-trivial higher order correlations in **Φ**

Measuring non-Gaussianity: halo abundance

Dark matter halos form in the peaks of the density field

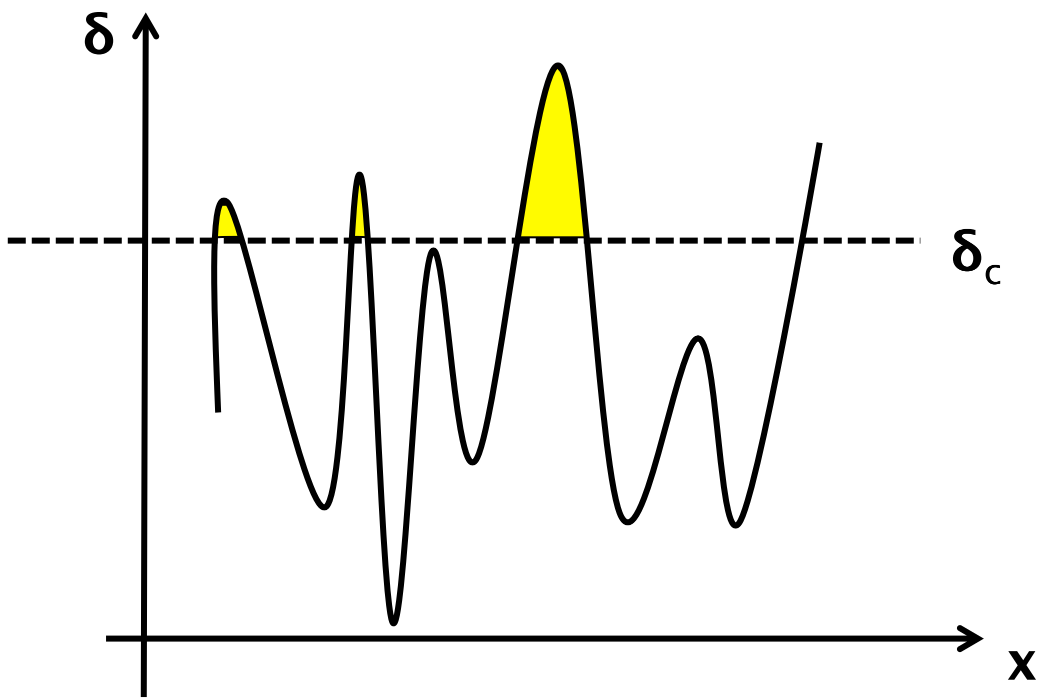

Non-Gaussianity changes the number density of the peaks

This in turn affects the halo mass function

Measuring non-Gaussianity: halo abundance

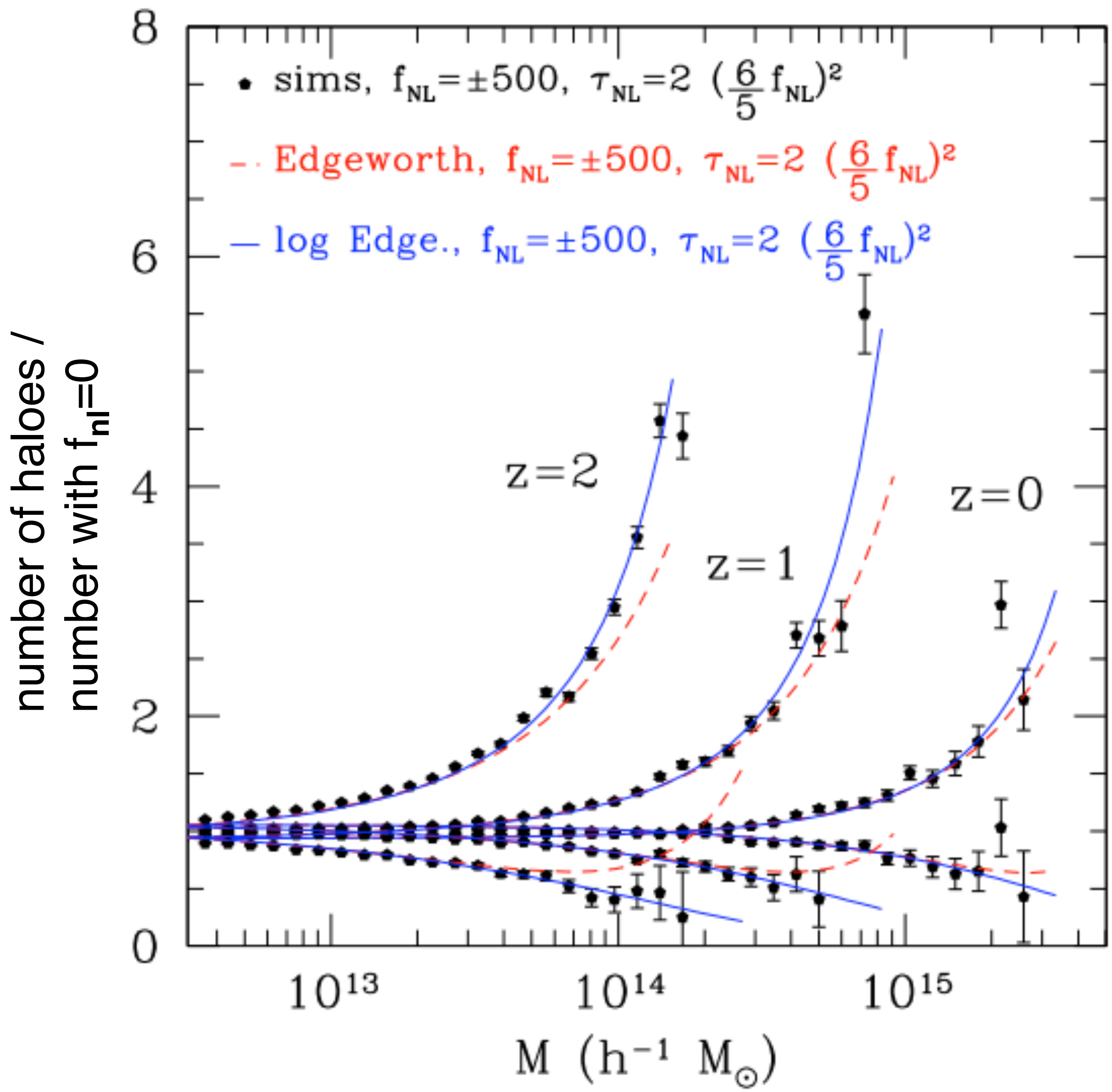

Largest effect is seen at highest masses

Insensitive to shape of bispectrum

But difficult to observe – relies on cluster masses being precisely known

LoVerde & Smith 2011, arXiv:1102.1439

Peak-background split bias model

Halo formation much easier with additional long-wavelength fluctuation

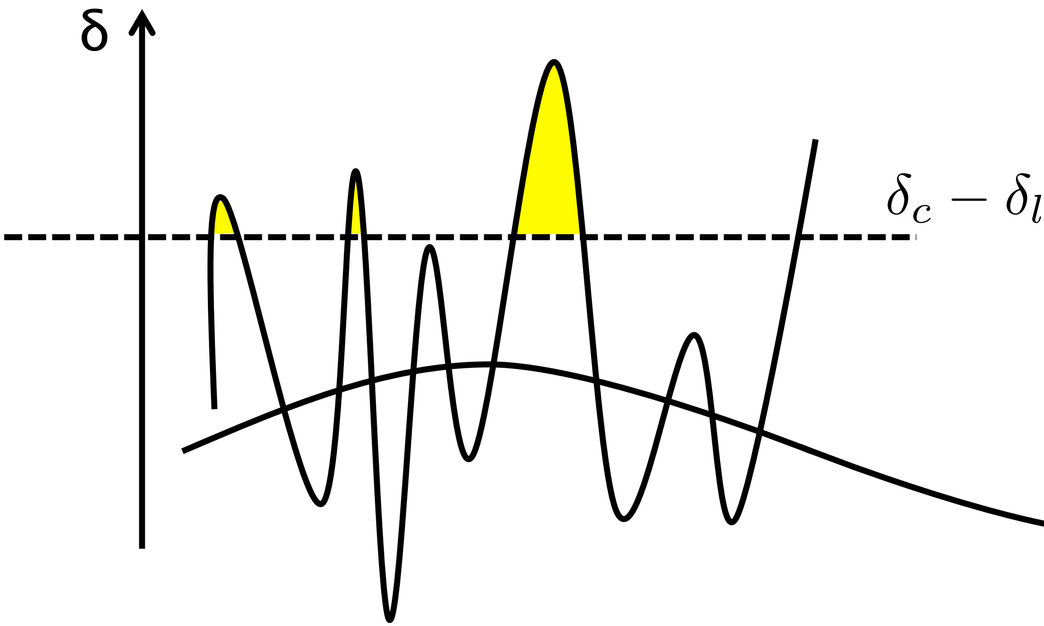

Number density of halos

$$n \to n - \frac{dn}{d\delta_c}\delta_l$$

Directly from the large-scale mode

Leads to a revised density $$(1+\delta_{\rm new}) = \left(1 + \frac{\Delta n}{n}\right)(1+\delta_l)$$

From the change in Number of haloes

To first order, this leads to a bias

$$\delta_{\rm new} = \left(\delta_l + \frac{\Delta n}{n}\right) \qquad b = \frac{\delta_{\rm new}}{\delta_l} = 1 + \frac{\Delta n}{n\delta_l} = 1 - \frac{d\ln n}{d\delta_c}$$

Peak-background split galaxy bias model

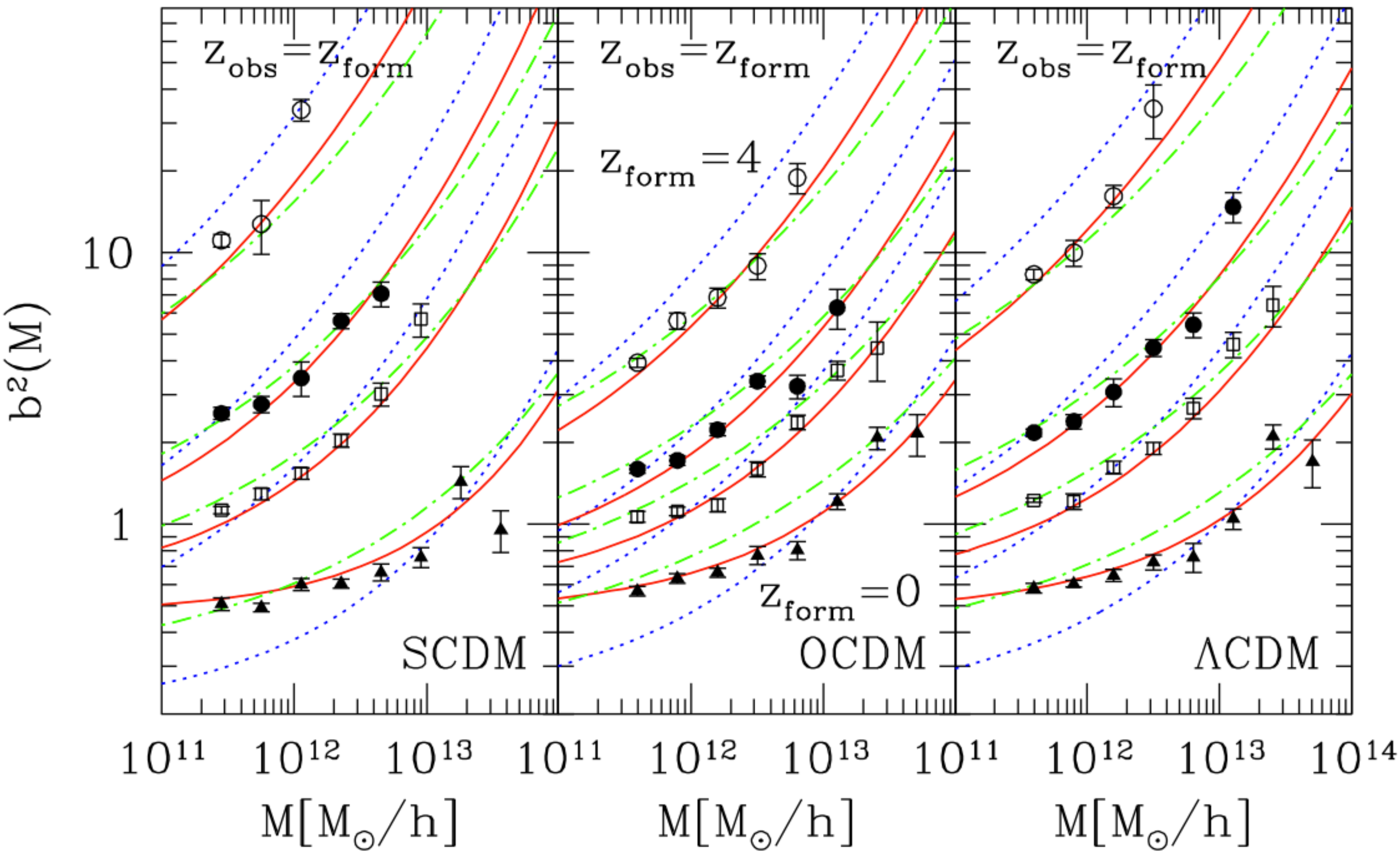

Sheth & Tormen 1999, arXiv:9901122

This is altered by f_{NL} signal

Now split non-Gaussian potential into long and short wavelength components

$$\Phi(\mathbf{x}) = \phi_l + \underbrace{f_{NL}\phi_l^2}_{\text{small}} + (1 + 2f_{NL}\phi_l)\phi_s + f_{NL}\phi_s^2 + \text{cnst}$$

Link between potential and overdensity field shows how changing long wavelength potential component changes "critical density"

$$\delta_l(k) = \alpha(k)\Phi(k) \quad \alpha(k) = \frac{2c^2k^2T(k)D(z)}{3\Omega_m H_0^2}$$

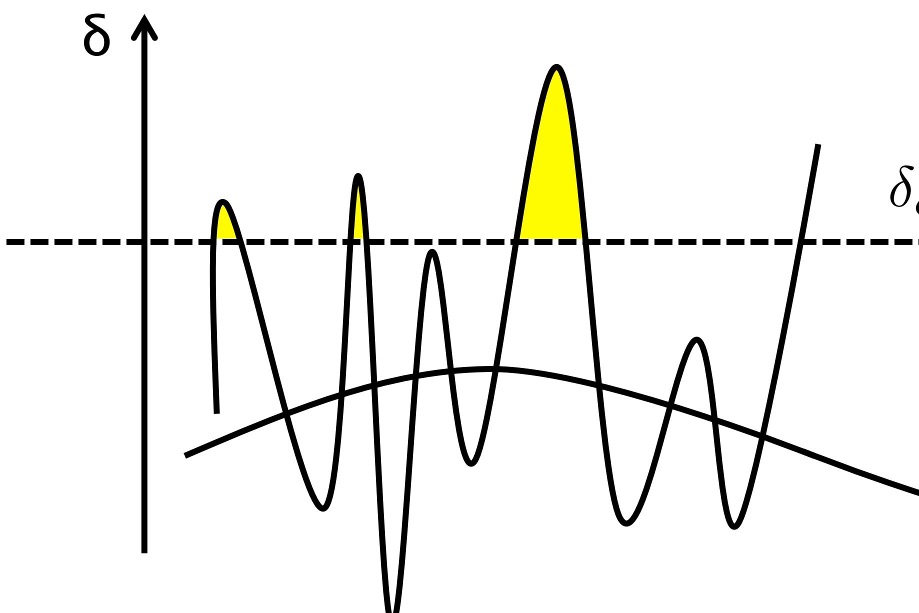

$$\delta_c - \delta_l - 2f_{NL}\phi_l = \delta_c - \delta_l\left(1 + \frac{2f_{NL}}{\alpha(k)}\right)$$

Peak-background split for non-Gaussianity

Halo formation much easier with additional long-wavelength fluctuation

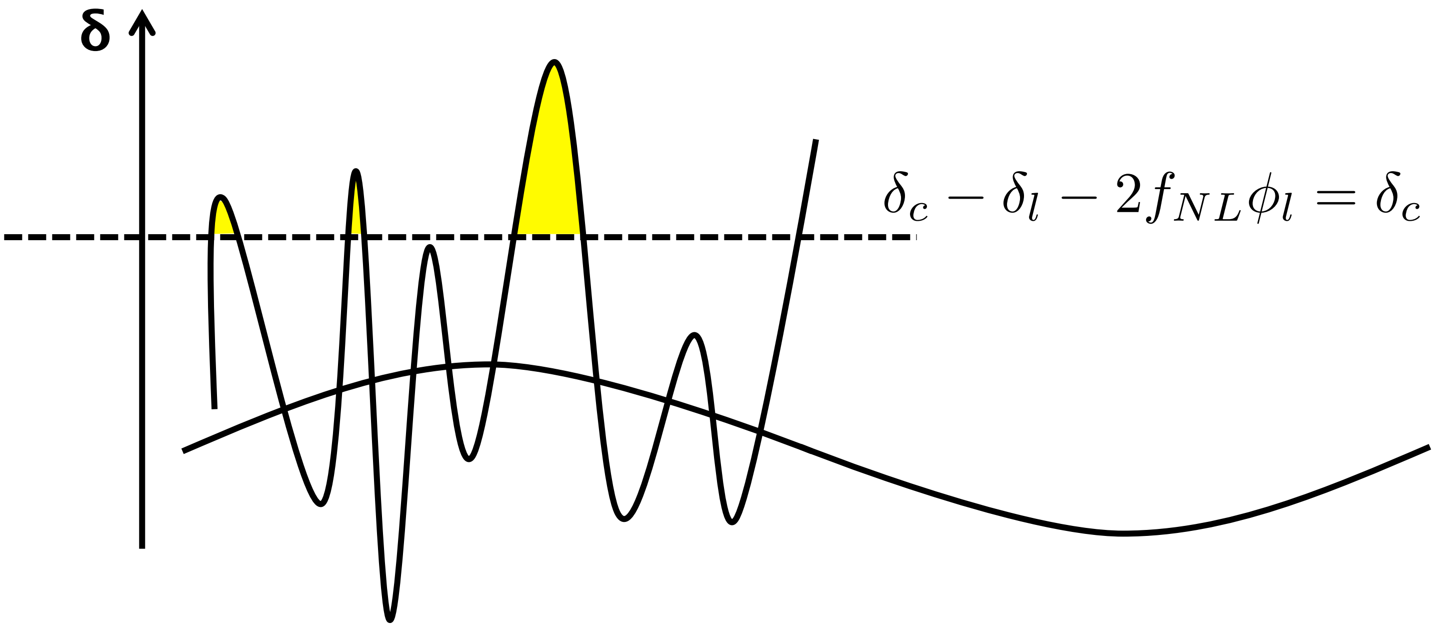

$$\delta_c - \delta_l - 2f_{NL}\phi_l = \delta_c - \delta_l\left(1 + \frac{2f_{NL}}{\alpha(k)}\right)$$

Number density of halos $\quad n \to n - \left(1 + \frac{2f_{NL}}{\alpha(k)}\right)\frac{dn}{d\delta_c}\delta_l$

Leads to a revised bias

$$b = 1 - \left(1 + \frac{2f_{NL}}{\alpha(k)}\right)\frac{d\ln n}{d\delta_c}$$

K^2 dependence in simulations

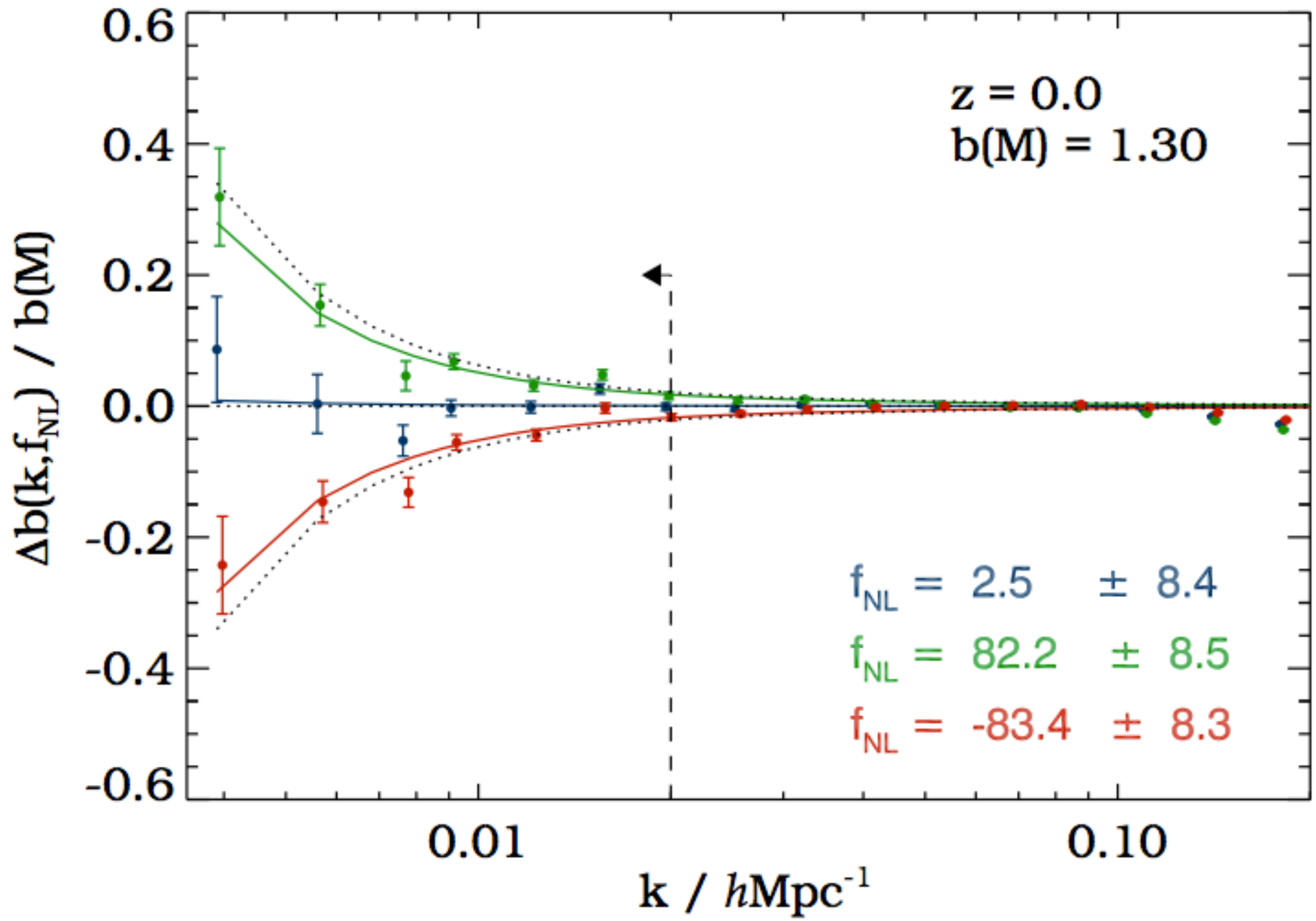

Dalal, Doré, Huterer, Shirokov 2007 ; Smith, LoVerde 2010; Smith, Ferraro, LoVerde 2011; Pillepich, Porciani, Hahn 2008; Desjacques, Seljak, Iliev 2008; Grossi et al 2009; Shandera, Dalal, Huterer 2010; Hamaus et al. 2011

Cosmology from surveys

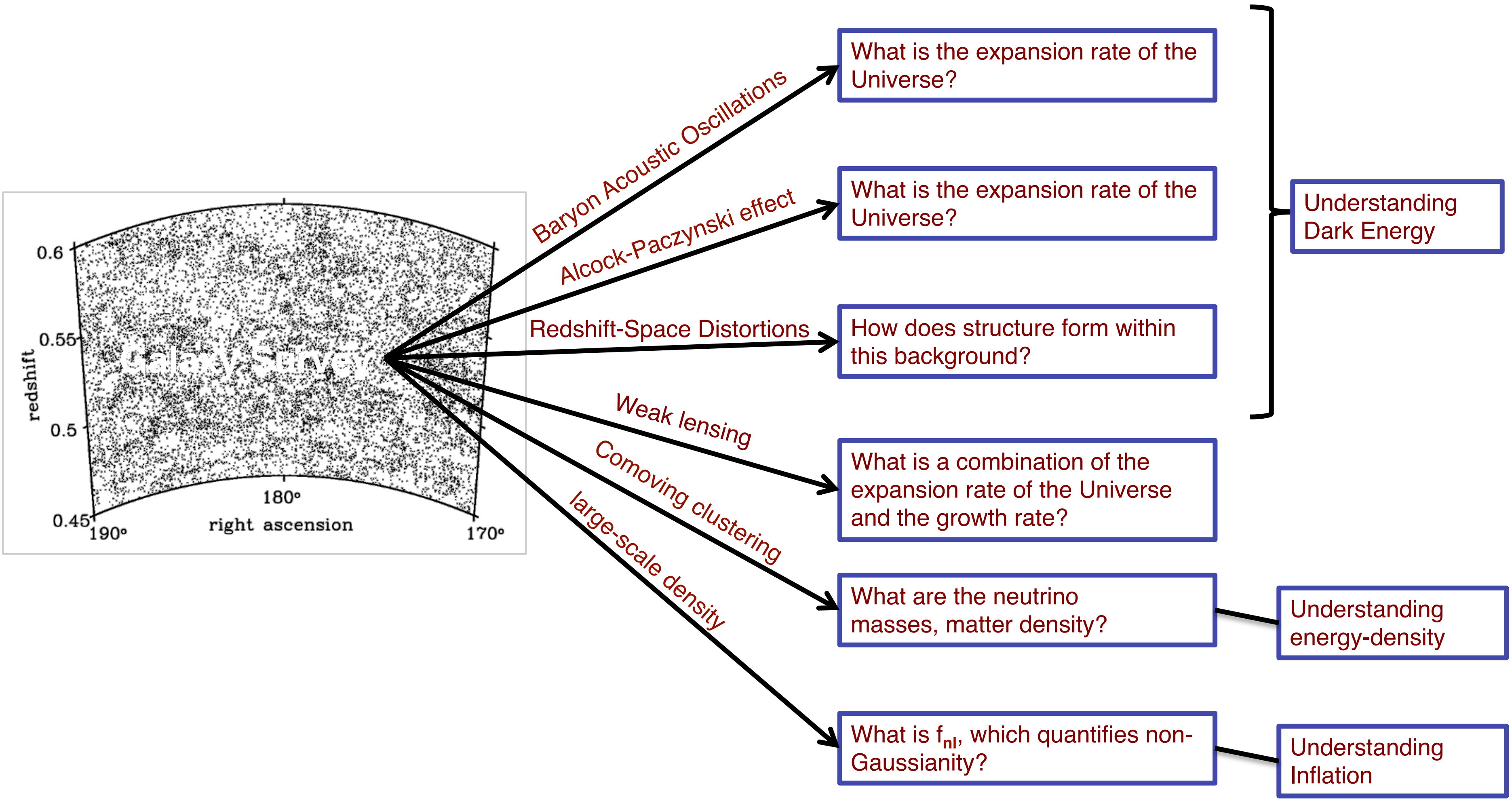

Future surveys: next 4-6 years

Dark Energy Survey (DES)

DARK ENERGY SURVEY

- New wide-field camera on the 4m Blanco telescope
- Survey underway, with first year of data in hand
- $\Omega = 5{,}000\mathrm{deg}^2$
- multi-colour optical imaging (g,r,i,z) with link to IR data from VISTA hemisphere survey
- 300,000,000 galaxies
- Aim is to constrain dark energy using 4 probes
  LSS/BAO, weak lensing, supernovae
  cluster number density
- Redshifts based on photometry
  weak radial measurements
  weak redshift-space distortions
- See also: Pan-STARRS, VST-VISTA, SkyMapper

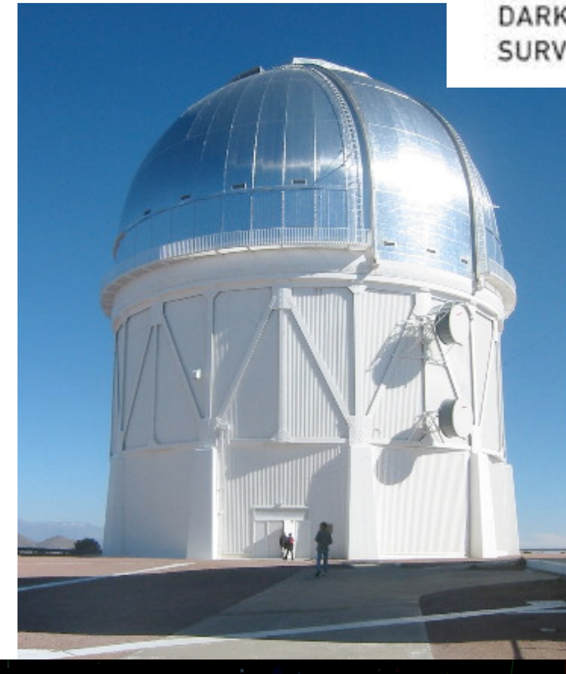

eBOSS / SDSS-IV

- The new cosmology project with SDSS
- Use the Sloan telescope and MOS to observe to higher redshift
- Basic parameters
  - Ω = 1,500deg^2 – 7,500deg^2
  - ~ 1,000,000 galaxies (direct BAO)
  - ~ 60,000 quasars (BAO from Ly-α forest)
- Distance measurements
  - 0.9% at z=0.8 (LRGs)
  - 1.8% at z=0.9 (ELGs)
  - 2.0% at z=1.5 (QSOs)
  - 1.1% at z=2.5 (Ly-α forest, inc. BOSS)
- Survey has just started, lasting 4--6 years
- Received $10M from Sloan foundation
  and significant funding from partners

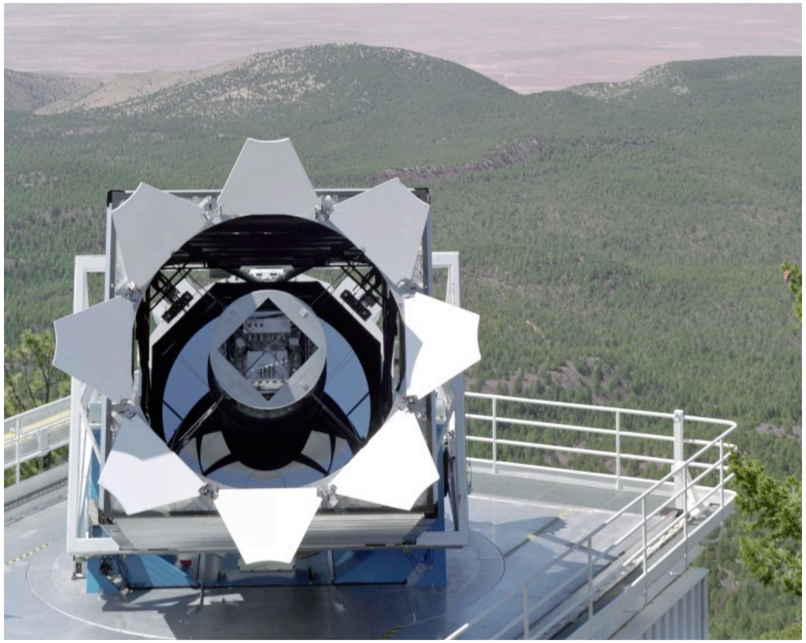

Future surveys: > 4 years

MOS on 4m-telescope

- New fibre-fed spectroscopes proposed
  for 4m telescopes
  - Mayall (BigBOSS) } DESI
  - Blanco (DESpec) } DESI
  - WHT (WEAVE)
  - VISTA (4MOST)
- Various stages of planning & funding
  - DESI has just passed DOE CD-1, 2019 start
  - 4MOST chosen by ESO, 2020 start?
  - WEAVE, 2018 start
- All capable of observing
  - Ω =5--14,000deg^2
  - 2--40,000,000 galaxies (direct BAO)
  - 1--600,000 quasars (BAO from Ly-α forest)
  - Cosmic variance limited to z ~ 1.4

MOS on 10m-telescope

- New fibre-fed spectroscopes proposed for 10m telescopes
  - Hobby-Eberly (HETDEX)
  - Subaru (PFS)
- Different baseline strategies
- HETDEX
  - 420deg^2 Ly-alpha emitters
  - 800,000 galaxies $1.9<z<3.5$
  - Greig, Komatsu & Wyithe, 2012, arXiv:12120977
- PFS
  - 1400deg^2 ELGs
  - 3,000,000 galaxies $0.6<z<2.4$
  - Ellis et al., 2012, arXiv:1206.0737

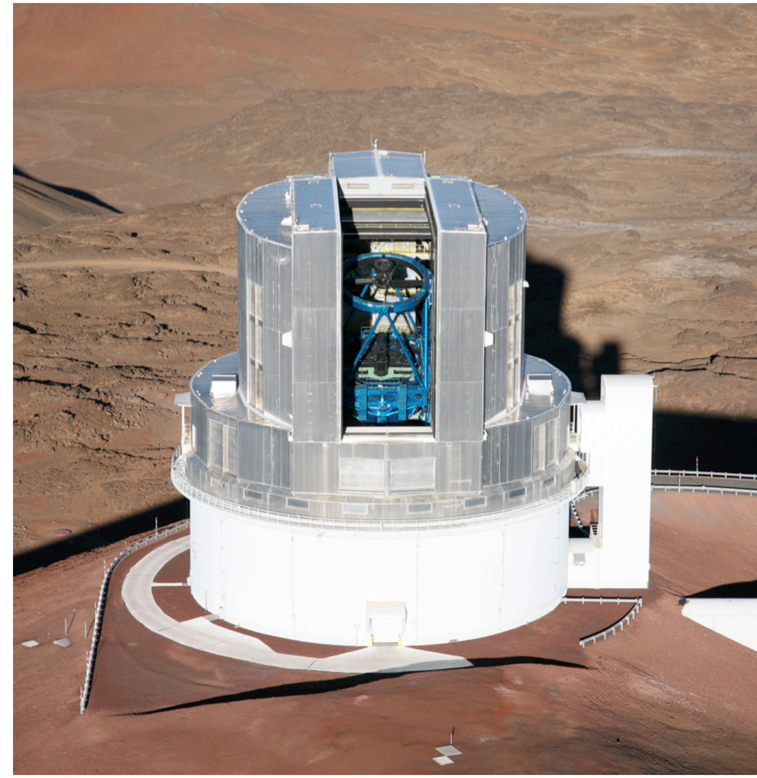

What is Euclid?

ESA Medium-Class mission
M2 slot in the Cosmic Visions Programme
Due for launch 2020

Scientific Objectives
To understand the origins of the Universe's accelerated expansion
Using at least 2 independent complementary probes

Geometry of the Universe
Weak Lensing (WL), Galaxy Clustering (BAO)

Cosmic history of structure formation
WL, Redshift-Space Distortions (RSD), Clusters of Galaxies (CL)

Using space-based observations to control residual systematic errors to an unprecedented low level

Euclid Consortium

The spacecraft & telescope

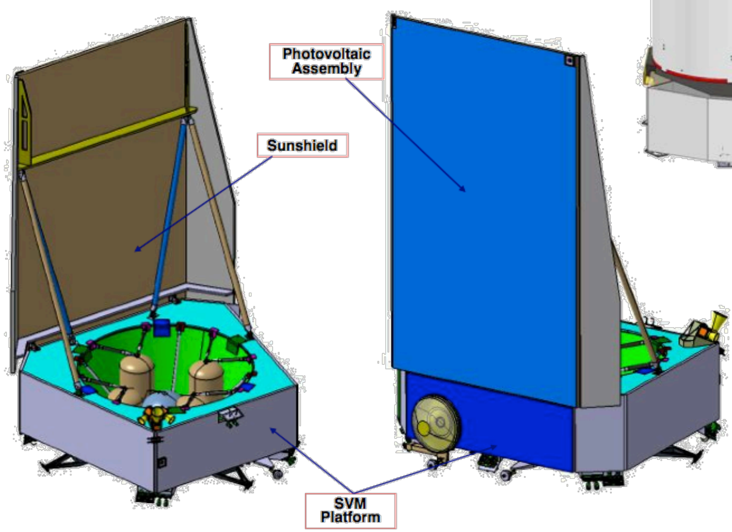

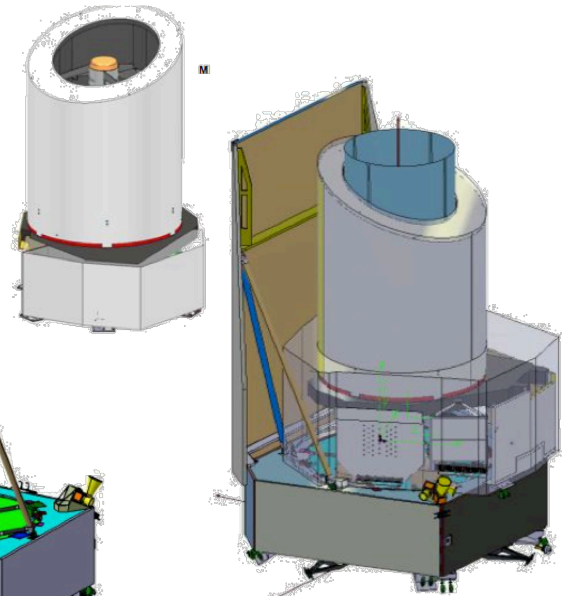

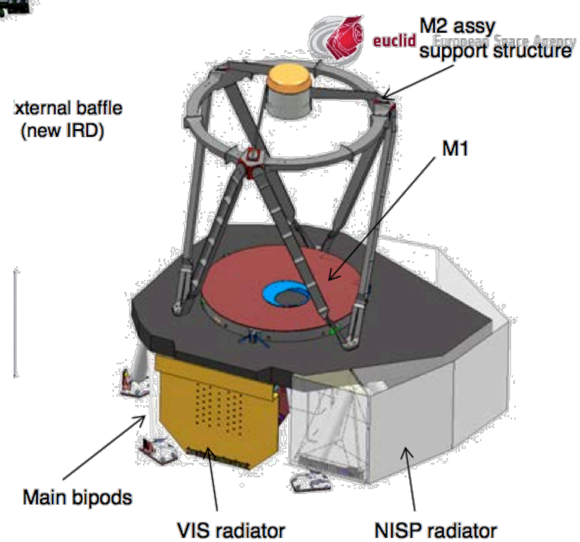

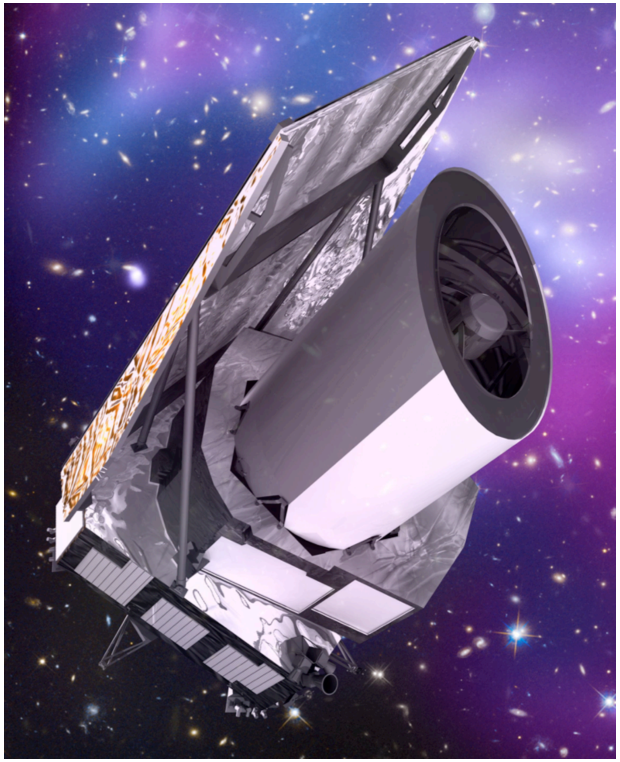

Euclid Consortium

The VIS instrument

Courtesy: S. Pottinger, R. Cole, M. Cropper and the VIS team

- 36 4kx4k CCDs with 12µm pixels
- 0.1 arcsec/pixel on sky
- 550-900nm (wide band channel)
- Lim. mag: AB 24.5 ; 10σ pt source
- Data volume:520 Gbit/day

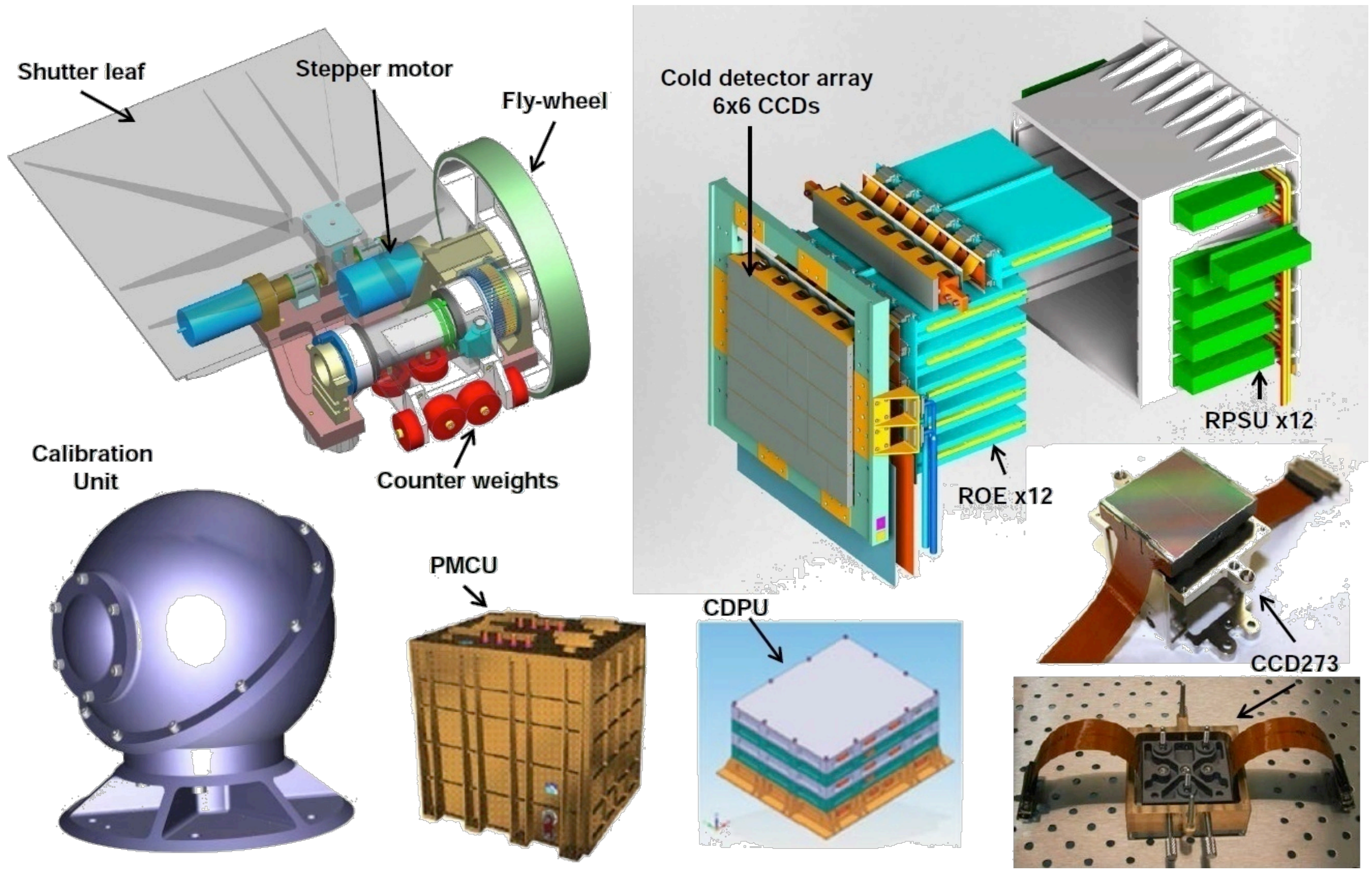

The NISP Instrument

Courtesy: T. Maciaszek and the NISP team

Structure Assembly & Thermal Control

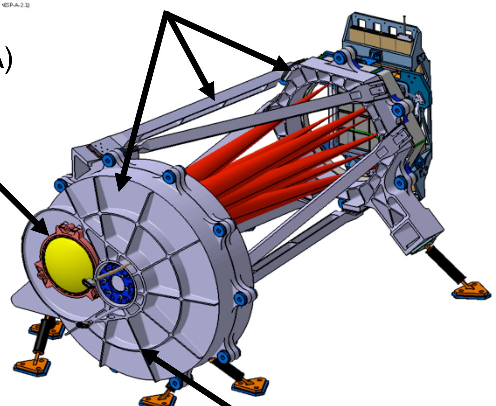

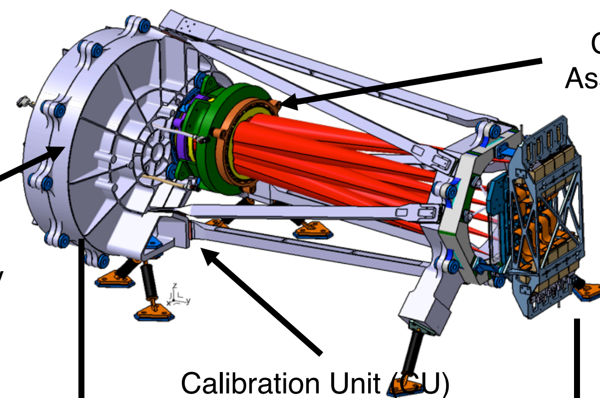

Temperature 140K

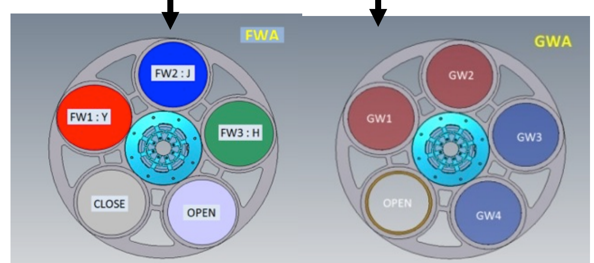

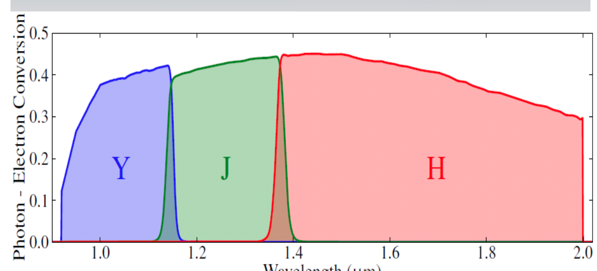

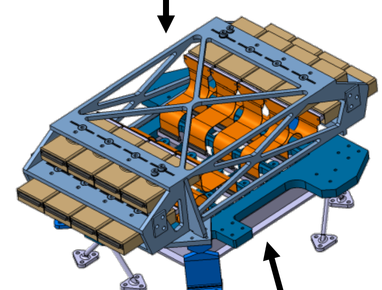

- 16 2kx2k H2GR NIR detectors
- 0.3 arcsec/pixel
- 3 NIR filters: H,J,K
- 4 Grisms (1 <B>; 3 <R>)
- Lim. mag: AB 24.0 ; 5σ pt source
- Data volume:180 Gbit/day

Euclid targets

Photo-z: Ground based Photometry and Spectroscopy

SURVEYS	In ~6 years	
	Area (deg2)	Description
Wide Survey	**15,000 deg²**	Step and stare with 4 dither pointings per step.
Deep Survey	**40 deg²**	In at least 2 patches of > 10 deg^2 2 magnitudes deeper than wide survey

PAYLOAD					
Telescope	1.2 m Korsch, 3 mirror anastigmat, f=24.5 m				
Instrument	VIS	NISP			
Field-of-View	0.787×0.709 deg^2	0.763×0.722 deg^2			
Capability	Visual Imaging	NIR Imaging Photometry			NIR Spectroscopy
Wavelength range	550– 900 nm	Y (920-1146nm),	J (1146-1372 nm)	H (1372-2000nm)	1100-2000 nm
Sensitivity	24.5 mag 10σ extended source	24 mag 5σ point source	24 mag 5σ point source	24 mag 5σ point source	$3\ 10^{-16}$ erg cm-2 s-1 3.5σ unresolved line flux
	Shapes + Photo-z of n = 1.5 x10^9 galaxies			***z* of n=2.6x10^7 galaxies**	

Possibility of other surveys: SN and/or m-lens surveys, Milky Way?

Euclid Definition Study Report: Laureijs et al arXiv:1110.3193

Euclid redshifts

Redshifts will be from slitless spectroscopy, mainly picking up H-α line

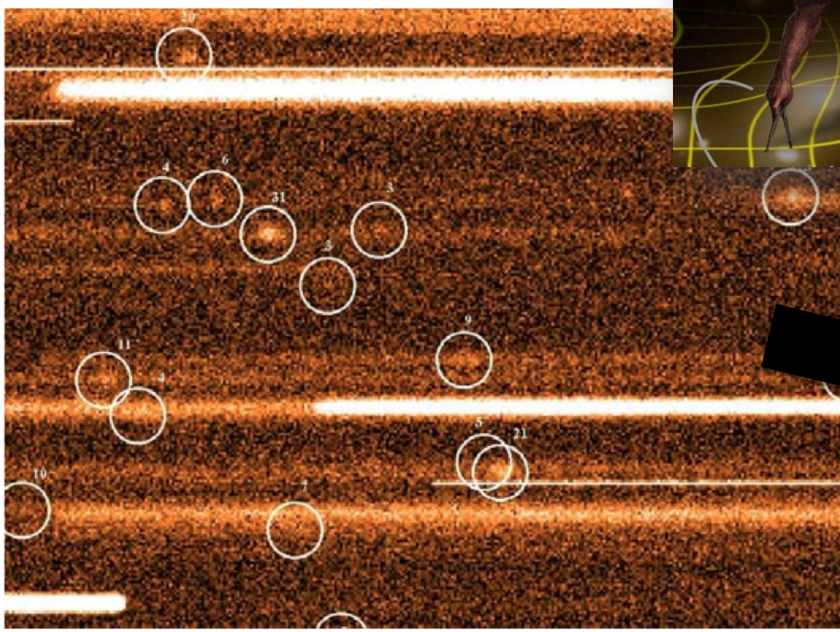

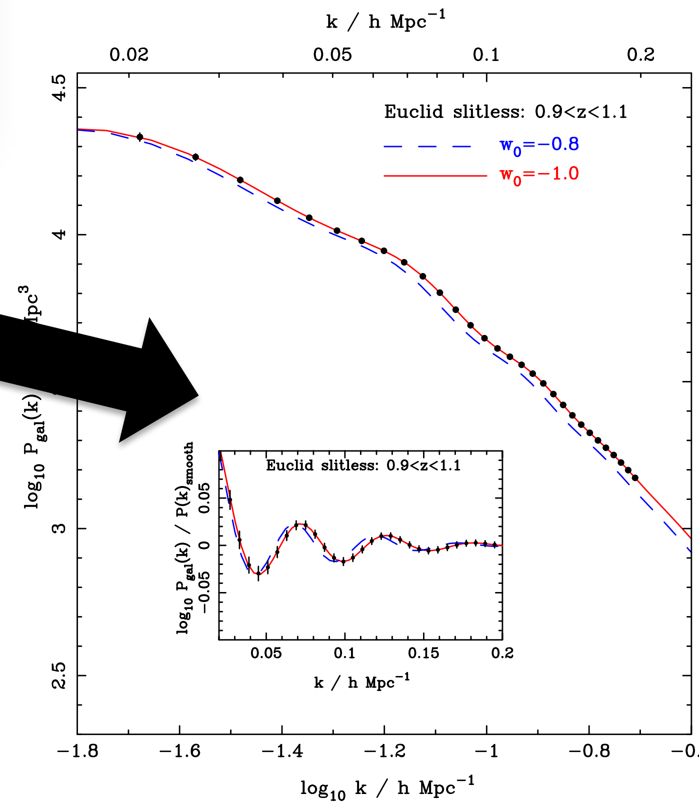

Long way from raw spectra to cosmology

Recent revision in Euclid strategy

Main motivations:
Evolving landscape: new surveys covering $z<1$ (e.g. eBOSS, DESI)

Revised estimates for density of H-alpha emitters

Instrument performance updates

Last chance to modify hardware/strategy to improve science and robustness

Systematic effects with slitless technique intrinsically hard to control

Outcome:
switch to strategy using grisms with single wavelength coverage

go deeper (2×10^{-16} erg cm^{-2} s^{-1}), but “only” over $0.9 < z < 1.8$

“expected yield” of 26M redshifts

BAO measurements for future surveys

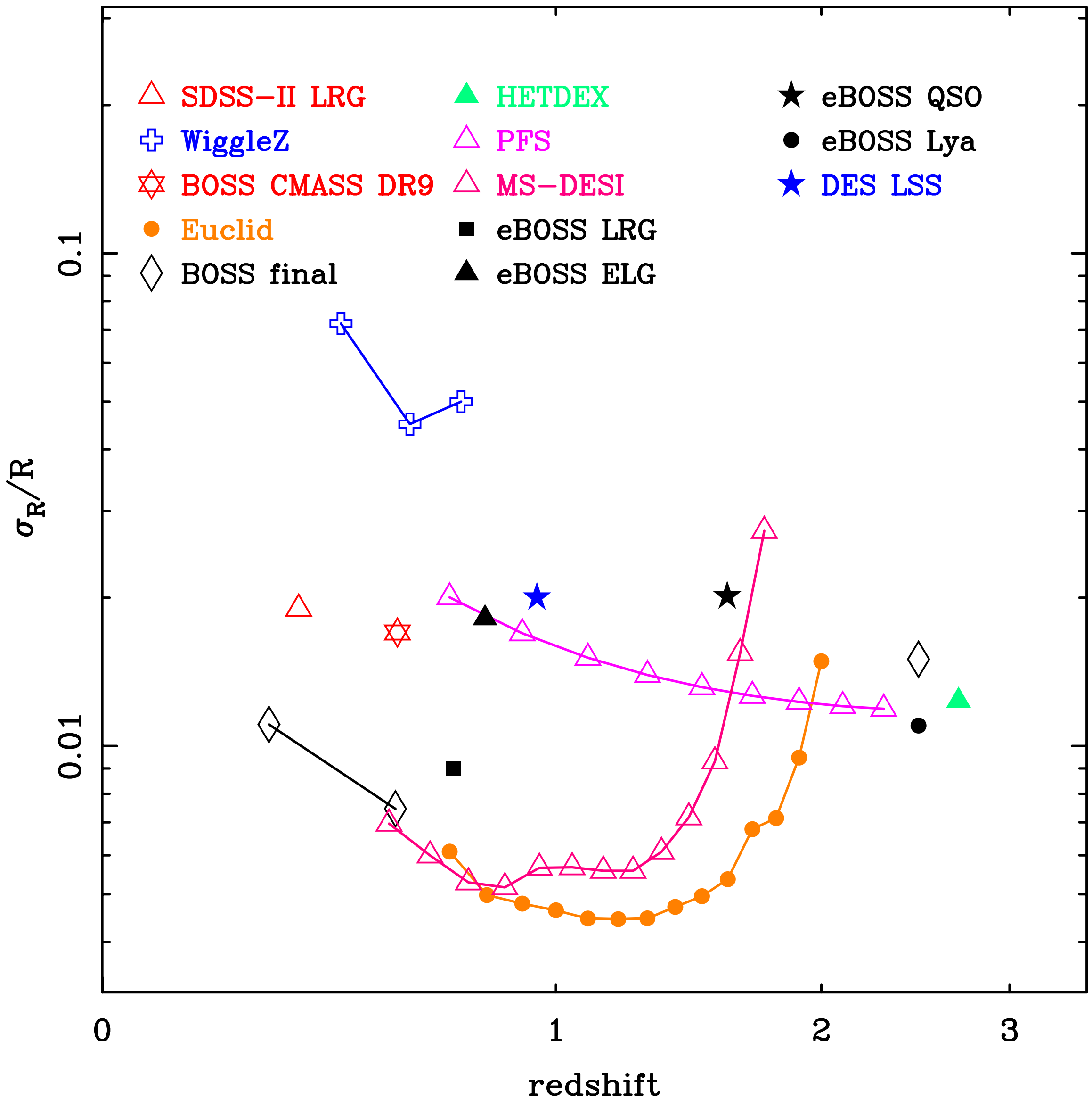

using the code of Seo & Eisenstein 2007, arXiv:0701079

BOSS CMASS DR9 galaxy clustering

BOSS CMASS galaxies at z~0.57

Total effective volume
V_{eff} = 2.2 Gpc^3

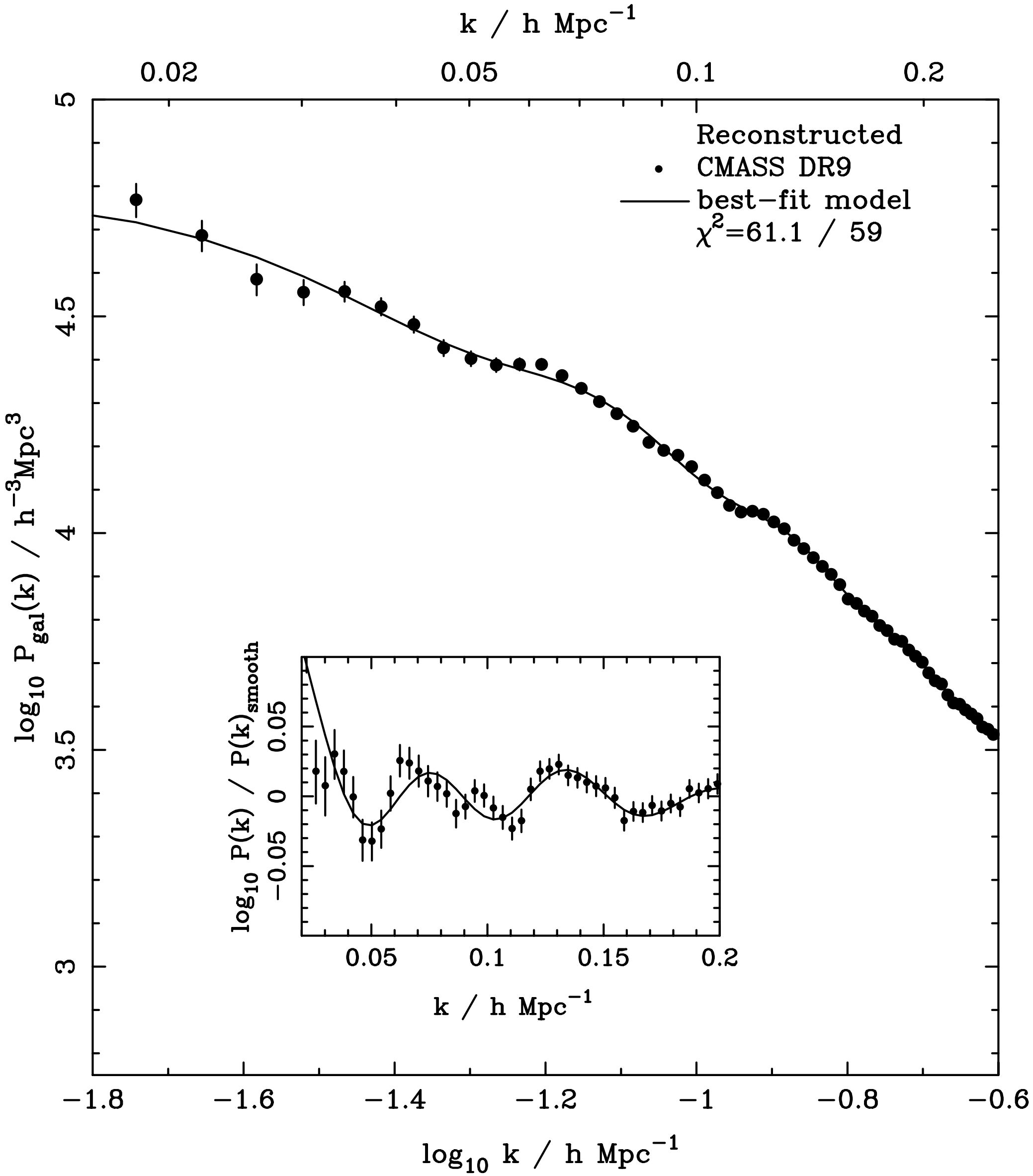

Anderson et al. 2012; arXiv:1203.6565

Predicted Euclid galaxy clustering

Redshift slice
0.9 < z < 1.1

Total effective volume (of Euclid)
$V_{\mathbf{eff}}$ = 57.4 Gpc^3

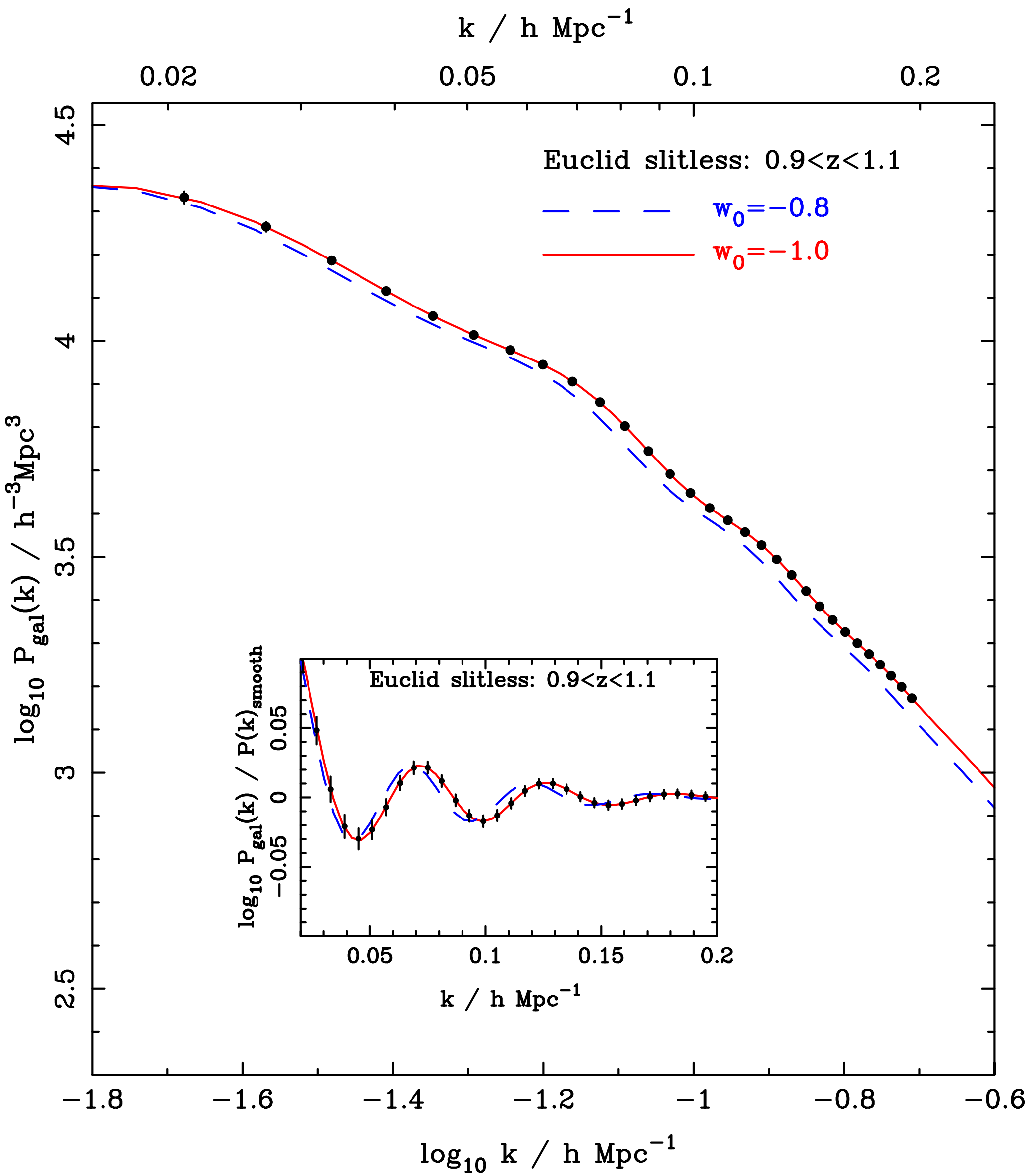

Improvement in precision

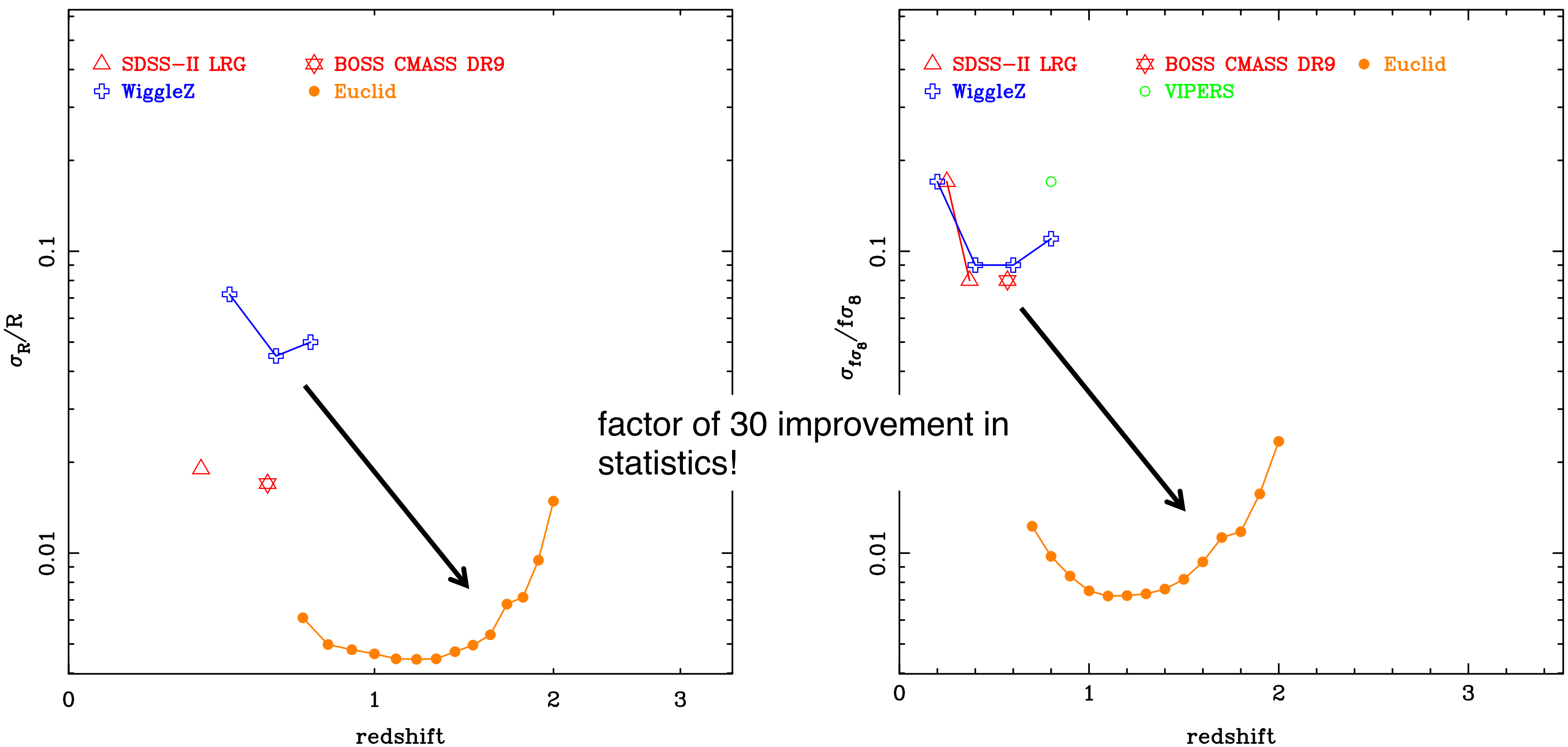

getting here relies on the low level of systematics in BAO emasurements…

Testing with subsamples

Testing with blue / red subsamples

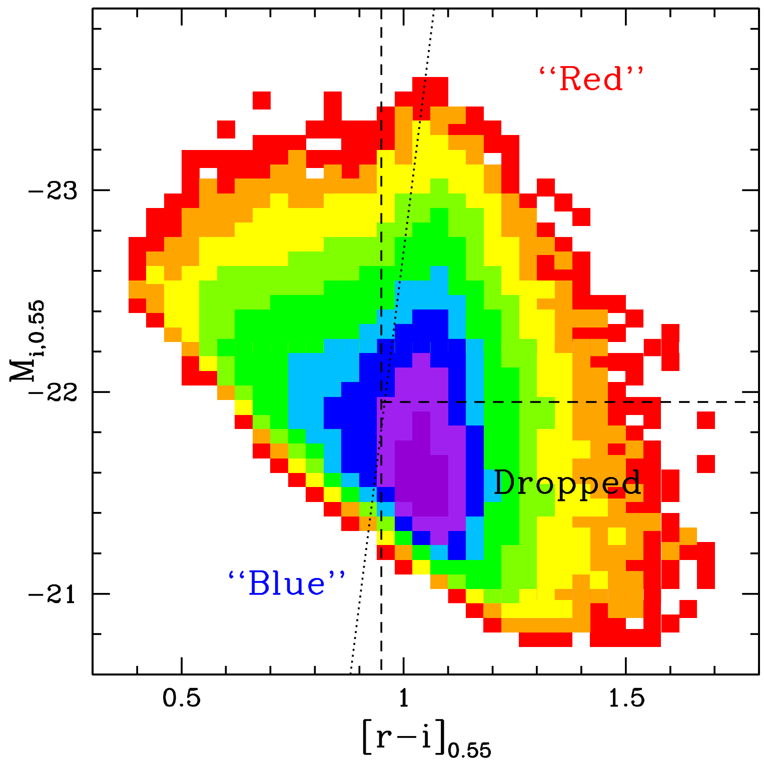

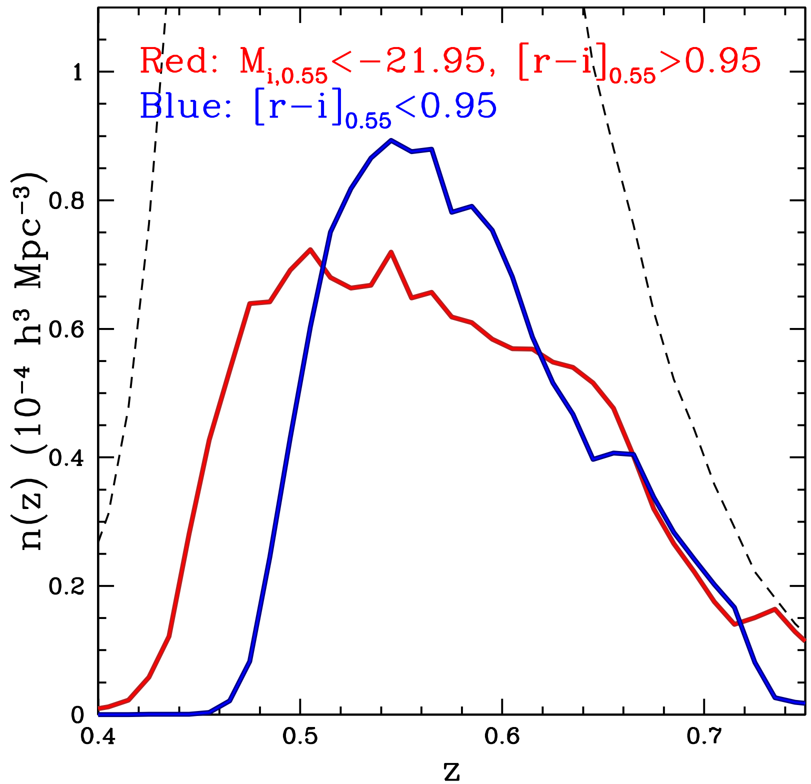

Ross et al. 2013, in prep

Testing with blue / red subsamples

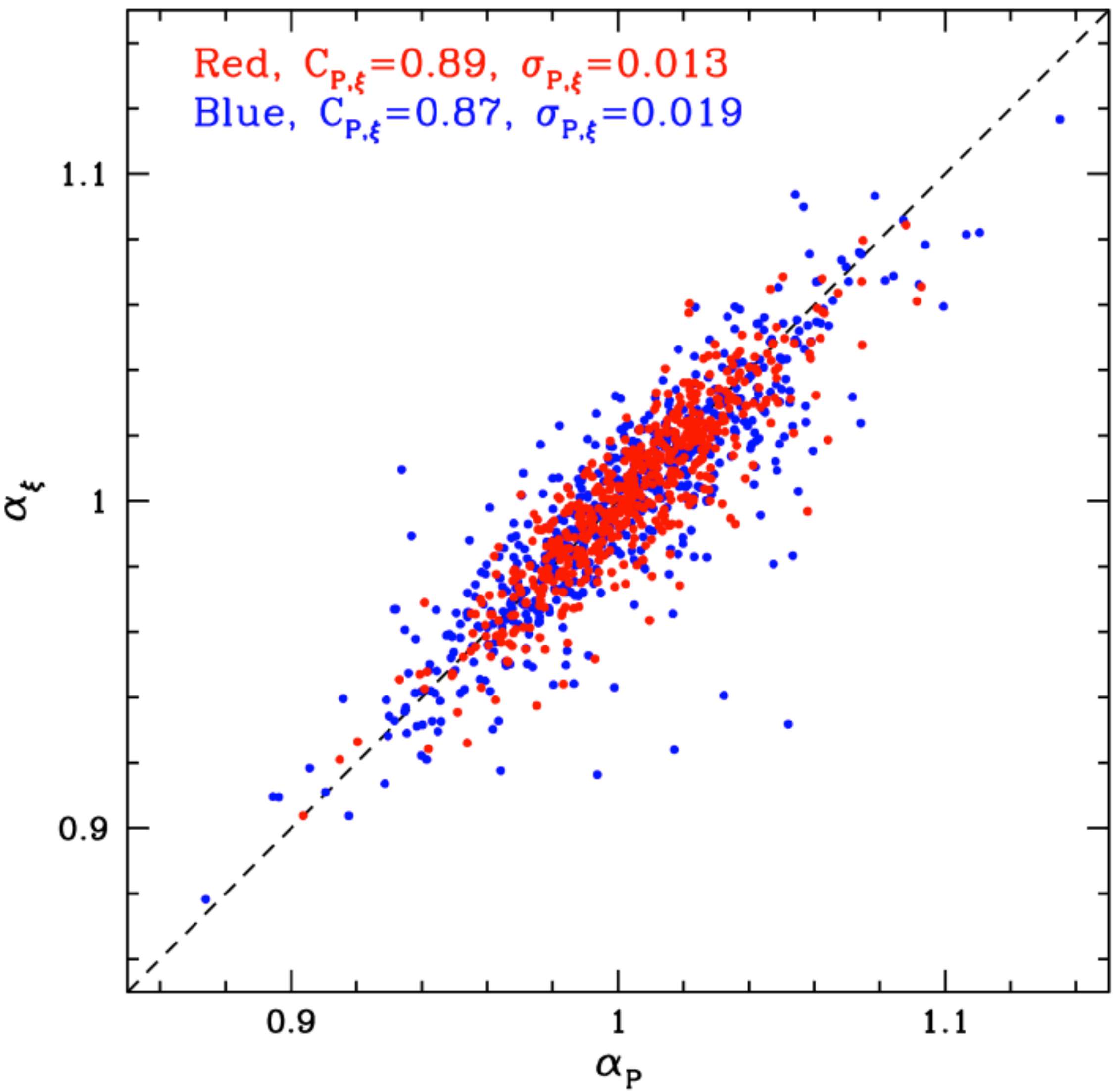

Ross et al. 2014, MNRAS 437, 1109

Getting the likelihood right

Getting the likelihood calculation 100% correct

The Likelihood under the standard assumption of a set of data drawn from a multi-variate Gaussian distribution is given by

$$\mathcal{L}(\mathbf{x}|\mathbf{p},\Psi^t) = \frac{|\Psi^t|}{\sqrt{2\pi}} \exp\left[-\frac{1}{2}\chi^2(\mathbf{x},\mathbf{p},\Psi^t)\right],$$

where $$\chi^2(\mathbf{x},\mathbf{p},\Psi^t) \equiv \sum_{ij} \left[x_i^d - x_i(\mathbf{p})\right] \Psi_{ij}^t \left[x_j^d - x_j(\mathbf{p})\right].$$

now suppose that the covariance matrix (size n_b x n_b) has been calculated from n_s simulations

$$\mu_i = \frac{1}{n_s}\sum_s x_i^s \qquad C_{ij} = \frac{1}{n_s - 1}\sum_s (x_i^s - \mu_i)(x_j^s - \mu_j)$$

then an unbiased estimator of the inverse covariance matrix is

$$\Psi = \frac{n_s - n_b - 2}{n_s - 1} C^{-1}$$

Hartlap J., Simon P., Schneider P., 2007, A&A, 464, 399

Errors in the covariance matrix

Simply providing an unbiased estimator of the inverse covariance matrix is not enough

The inverse covariance matrix also has its own error

$$\langle \Delta\Psi_{ij} \Delta\Psi_{i'j'} \rangle = A \Psi_{ij} \Psi_{i'j'} + B(\Psi_{ii'} \Psi_{jj'} + \Psi_{ij'} \Psi_{ji'}),$$

$$A = \frac{2}{(n_s - n_b - 1)(n_s - n_b - 4)}$$

$$B = \frac{(n_s - n_b - 2)}{(n_s - n_b - 1)(n_s - n_b - 4)}$$

Strictly, we should form a joint likelihood

$$\mathcal{L}(\mathbf{x}, \Psi | \mathbf{p}, \Psi^t) = \mathcal{L}(\mathbf{x} | \mathbf{p}, \Psi) \mathcal{L}(\Psi | \Psi^t),$$

If we don't, this leads to an additional error on the $n_\mathbf{p}$ parameters being fitted

$$\langle p_\alpha p_\beta \rangle |_{s.o.} = B(n_b - n_p) F^{-1}_{\alpha\beta},$$

Taylor et al., 2012, arXiv:1212.4359; Dodelson & Schneider 2007, arXiv:1212.4359

Getting the model right

BAO from simulations

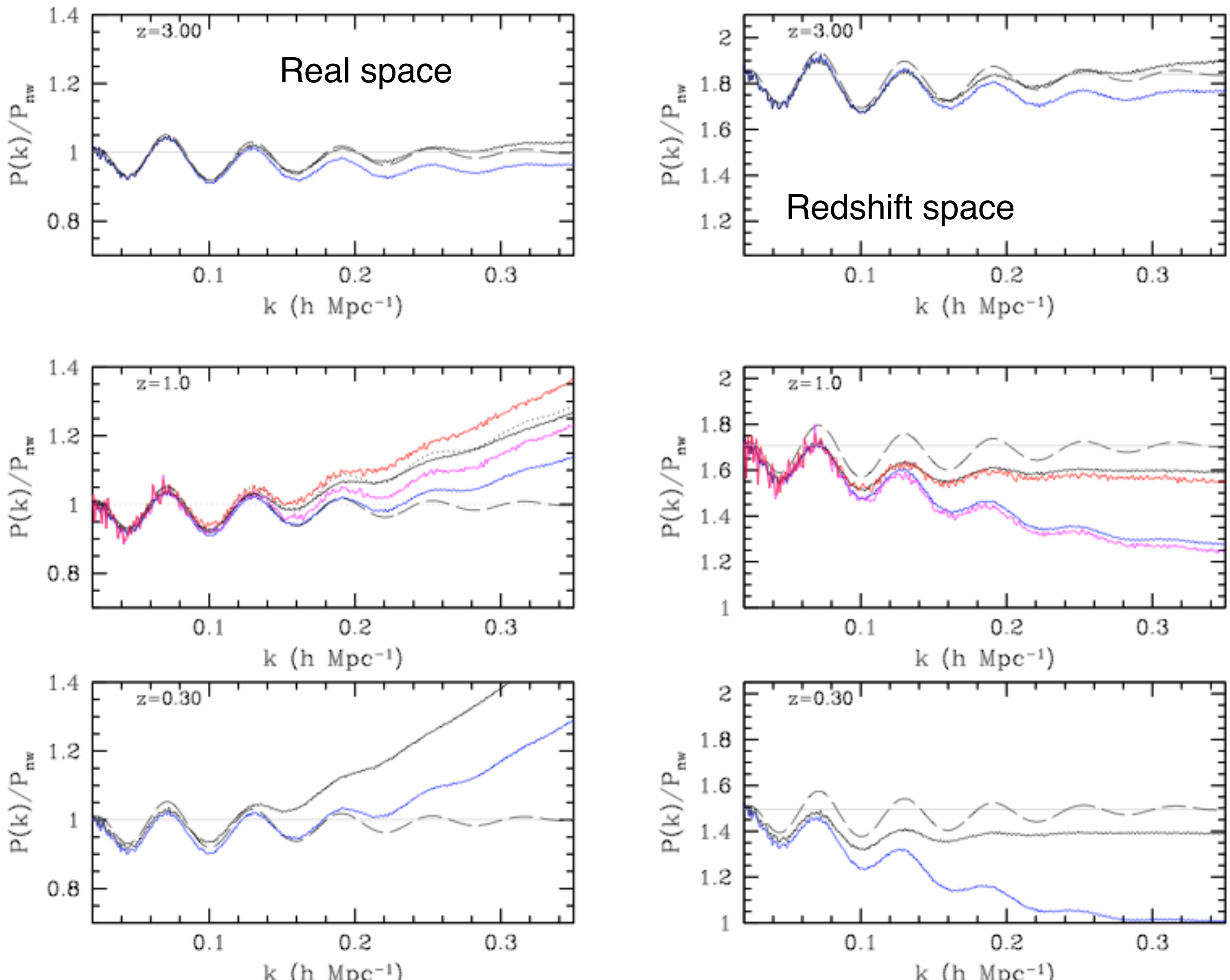

Seo et al., 2010, arXiv:0910.5005

BAO from simulations

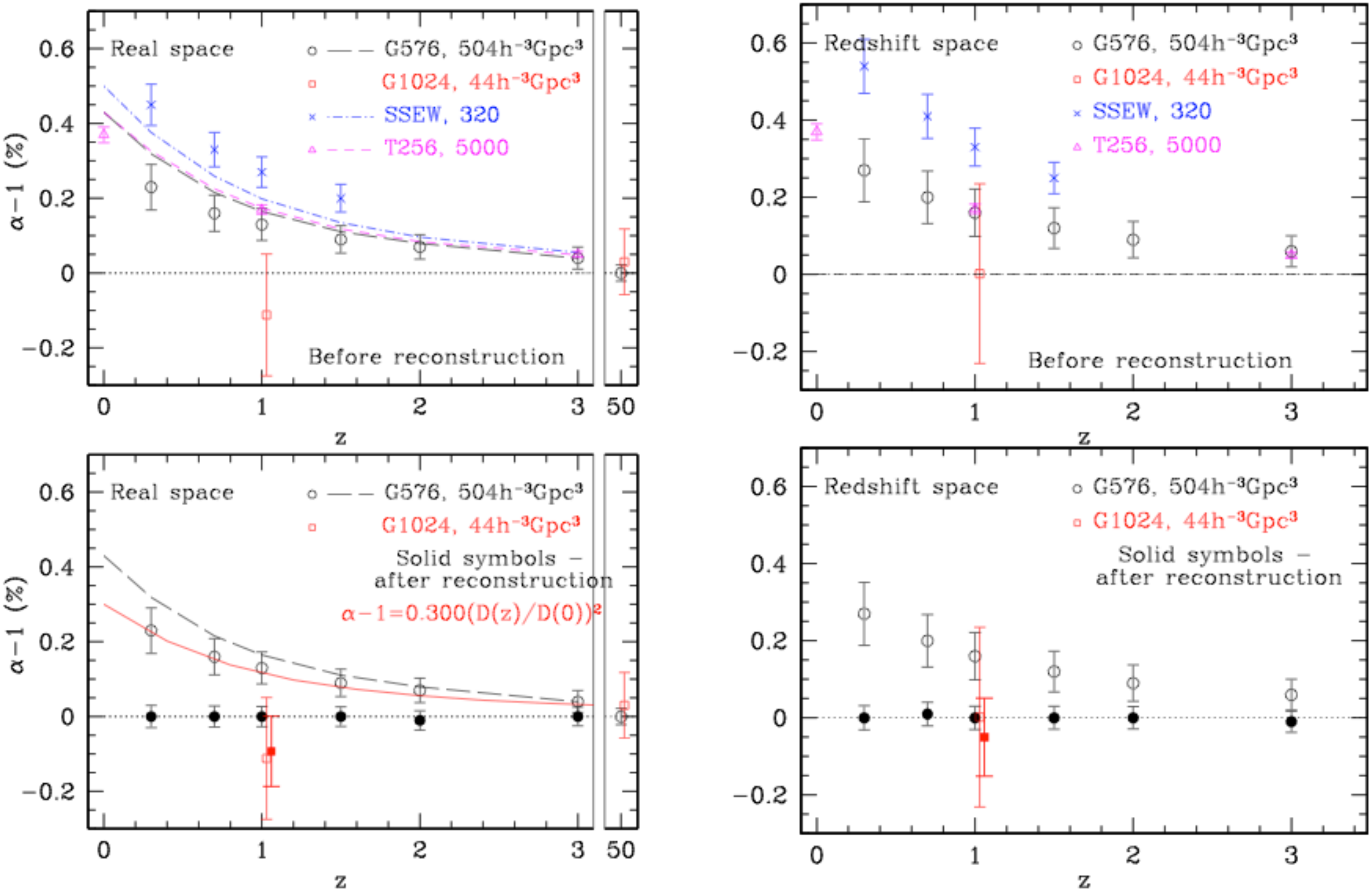

Seo et al., 2010, arXiv:0910.5005

What will you be showing in 15 years time?

At the same time as my PhD …

Photo: U. Montan

Saul Perlmutter

Photo: U. Montan

Brian P. Schmidt

Photo: U. Montan

Adam G. Riess

The Nobel Prize in Physics 2011 was divided, one half awarded to Saul Perlmutter, the other half jointly to Brian P. Schmidt and Adam G. Riess *"for the discovery of the accelerating expansion of the Universe through observations of distant supernovae"*.

SDSS-II LRG BAO vs other data

ΛCDM models with curvature

flat wCDM models

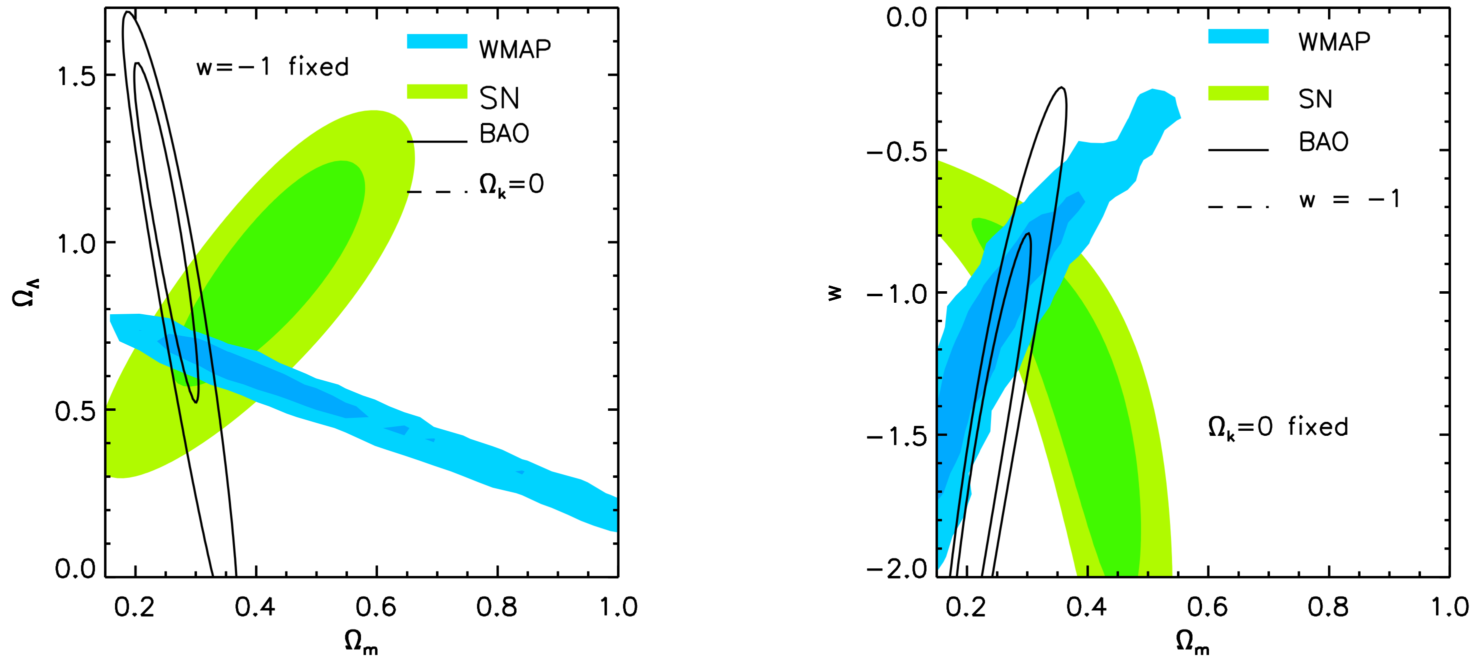

Union supernovae

WMAP 5year

SDSS-II BAO Constraint on $r_s(z_d)/D_V(0.2)$ & $r_s(z_d)/D_V(0.35)$

Percival et al. 2009; arXiv:0907.1660

Euclid BAO predictions

ΛCDM models with curvature

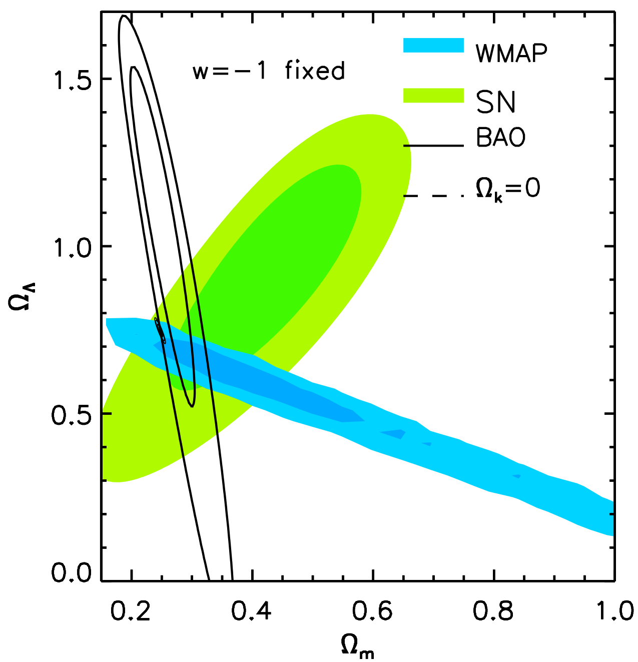

flat wCDM models

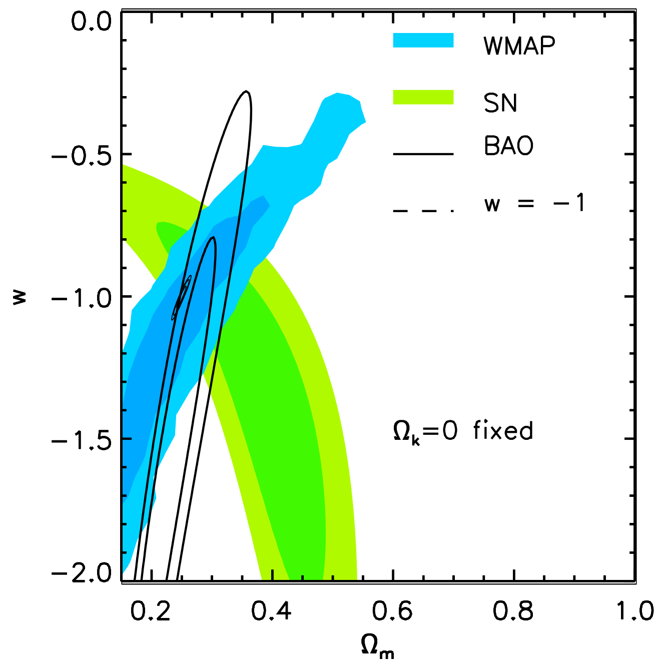

Union supernovae

WMAP 5year

SDSS-II BAO Constraint on $r_s(z_d)/D_V(0.2)$ & $r_s(z_d)/D_V(0.35)$

Cosmology from surveys